
Article:
Bryant, D. J., Nelson, B. S. orcid.org/0000-0003-4493-4086, Swift, S. J. et al. (17 more authors) (2023) Biogenic and anthropogenic sources of isoprene and monoterpenes and their secondary organic aerosol in Delhi, India. Atmospheric Chemistry and Physics. pp. 61-83. ISSN 1680-7324

https://doi.org/10.5194/acp-23-61-2023

Atmos. Chem. Phys., 23, 61–83, 2023
https://doi.org/10.5194/acp-23-61-2023

Atmospheric Chemistry and Physics
Open Access
EGU

Biogenic and anthropogenic sources of isoprene and monoterpenes and their secondary organic aerosol in Delhi, India

Daniel J. Bryant[1], Beth S. Nelson[1], Stefan J. Swift[1,a], Sri Hapsari Budisulistiorini[1], Will S. Drysdale[1,2], Adam R. Vaughan[1], Mike J. Newland[1,b], James R. Hopkins[1,2], James M. Cash[3,4], Ben Langford[3], Eiko Nemitz[3], W. Joe F. Acton[5,c], C. Nicholas Hewitt[5], Tuhin Mandal[6], Bhola R. Gurjar[6], Shivani[6,d], Ranu Gadi[6], James D. Lee[1,2], Andrew R. Rickard[1,2], and Jacqueline F. Hamilton[1]

[1]Wolfson Atmospheric Chemistry Laboratories, Department of Chemistry, University of York, Heslington, York, YO10 5DD, UK
[2]National Centre for Atmospheric Science, University of York, Heslington, York, YO10 5DD, UK
[3]UK Centre for Ecology and Hydrology, Penicuik, Midlothian, Edinburgh, EH26 0QB, UK
[4]School of Chemistry, University of Edinburgh, Edinburgh, EH9 3FJ, Edinburgh, UK
[5]Lancaster Environment Centre, Lancaster University, Lancaster, LA1 4YW, UK
[6]Department of Applied Sciences and Humanities, Indira Gandhi Delhi Technical University for Women, Delhi, 110006, India
[a]now at: J. Heyrovsky Institute of Physical Chemistry, Department of Chemistry of Ions in Gaseous Phase, Prague, Czech Republic
[b]now at: ICARE-CNRS, 1 C Av. de la Recherche Scientifique, 45071 Orléans CEDEX 2, France
[c]now at: School of Geography, Earth and Environmental Sciences, University of Birmingham, Birmingham, B15 2TT, UK
[d]now at: Department of Chemistry, Miranda House, Delhi University, Delhi, 110007, India

Correspondence: Daniel J. Bryant (daniel.bryant@york.ac.uk)

Received: 24 August 2022 – Discussion started: 14 September 2022
Revised: 16 November 2022 – Accepted: 29 November 2022 – Published: 3 January 2023

Abstract. Isoprene and monoterpene emissions to the atmosphere are generally dominated by biogenic sources. The oxidation of these compounds can lead to the production of secondary organic aerosol; however the impact of this chemistry in polluted urban settings has been poorly studied. Isoprene and monoterpenes can form secondary organic aerosol (SOA) heterogeneously via anthropogenic–biogenic interactions, resulting in the formation of organosulfate (OS) and nitrooxy-organosulfate (NOS) species. Delhi, India, is one of the most polluted cities in the world, but little is known about the emissions of biogenic volatile organic compounds (VOCs) or the sources of SOA. As part of the DELHI-FLUX project, gas-phase mixing ratios of isoprene and speciated monoterpenes were measured during pre- and post-monsoon measurement campaigns in central Delhi. Nocturnal mixing ratios of the VOCs were substantially higher during the post-monsoon (isoprene: (0.65 ± 0.43) ppbv; limonene: (0.59 ± 0.11) ppbv; α-pinene: (0.13 ± 0.12) ppbv) than the pre-monsoon (isoprene: (0.13 ± 0.18) ppbv; limonene: 0.011 ± 0.025 (ppbv); α-pinene: 0.033 ± 0.009) period. At night, isoprene and monoterpene concentrations correlated strongly with CO during the post-monsoon period. Filter samples of particulate matter less than 2.5 µm in diameter ($PM_{2.5}$) were collected and the OS and NOS content analysed using ultra-high-performance liquid chromatography tandem mass spectrometry (UHPLC-MS^2). Inorganic sulfate was shown to facilitate the formation of isoprene OS species across both campaigns. Sulfate contained within OS and NOS species was shown to contribute significantly to the sulfate signal measured via AMS. Strong nocturnal enhancements of NOS species were observed across both campaigns. The total concentration of OS and NOS species contributed an average of (2.0 ± 0.9) % and (1.8 ± 1.4) % to the total oxidized organic aerosol and up to a maximum of 4.2 % and 6.6 %

across the pre- and post-monsoon periods, respectively. Overall, this study provides the first molecular-level measurements of SOA derived from isoprene and monoterpene in Delhi and demonstrates that both biogenic and anthropogenic sources of these compounds can be important in urban areas.

1 Introduction

India is undergoing significant urbanization and industrialization, with a rapidly increasing population. India is home to 14 out of the top 20 most polluted cities in the world between 2017 and 2021 in terms of annual mean $PM_{2.5}$ (particulate matter less than 2.5 µm in diameter) concentrations. In Delhi, the population-weighted mean $PM_{2.5}$ was estimated to be 209 $\mu g\,m^{-3}$ (range: 120–339.5 $\mu g\,m^{-3}$) in 2017, over 40 times the WHO annual mean guidelines of 5 $\mu g\,m^{-3}$ and greater than 5 times India's own standard of 40 $\mu g\,m^{-3}$ (Balakrishnan et al., 2019). Air pollution is estimated to cause over 1 million deaths per year in India alone (Landrigan et al., 2018).

Numerous studies have investigated $PM_{2.5}$ concentrations, characteristics, and meteorological effects in Delhi (Anand et al., 2019; Bhandari et al., 2020; Chowdhury et al., 2004; Hama et al., 2020; Kanawade et al., 2020; Miyazaki et al., 2009; Nagar et al., 2017). The key sources of $PM_{2.5}$ identified are secondary aerosol, fossil fuel combustion, municipal waste, and biomass burning (Chowdhury et al., 2004; Sharma and Mandal, 2017; Stewart et al., 2021a, b). Previous studies have also shown that alongside extremely high emissions of pollutants, regional sources and meteorology in particular play an important role in high-pollution events in Delhi (Bhandari et al., 2020; Sawlani et al., 2019; Schnell et al., 2018; Sinha et al., 2014).

Secondary species have been shown to be significant contributors to PM_1 and $PM_{2.5}$ mass in Delhi, with organics contributing 40 %–70 % of PM_1 mass (Gani et al., 2019; Shivani et al., 2019; Reyes-Villegas et al., 2021; Sharma and Mandal, 2017). However, limited molecular-level analysis of organic aerosol (OA) has been undertaken (Chowdhury et al., 2004; Elzein et al., 2020; Miyazaki et al., 2009; Singh et al., 2021, 2012; Yadav et al., 2021). Kirillova et al. (2014) analysed the sources of water-soluble organic carbon (WSOC) in Delhi, using radiocarbon measurement constraints. The study identified that 79 % of WSOC was classified as non-fossil carbon, attributed to biogenic and biomass burning sources in urban Delhi (Kirillova et al., 2014), similar to other studies from India (Kirillova et al., 2013; Sheesley et al., 2012). Studies across Asia, Europe, and North America have also shown high contributions from non-fossil sources to ambient PM concentrations in urban environments (Du et al., 2014; Kirillova et al., 2010; Szidat et al., 2004; Wozniak et al., 2012). The sources of this modern carbon in urban areas are poorly understood, although biomass burning is a key component (Elser et al., 2016; Hu et al., 2016; Lanz et al., 2010; Nagar et al., 2017). Recently in Delhi, solid-fuel combustion sources such as cow dung cake or municipal solid waste have been shown to release over 1000 different organic components into the aerosol phase at emission (Stewart et al., 2021b). Alongside biomass burning, one potential source of this non-fossil aerosol is biogenic secondary organic aerosol (BSOA), which is formed via the oxidation of biogenic volatile organic compounds (BVOCs) and subsequent gas–particle phase transfer (Hallquist et al., 2009; Hoffmann et al., 1997).

Isoprene is the most abundant BVOC, with annual global emissions estimates of between 350–800 $Tg\,yr^{-1}$ (Guenther et al., 2012; Sindelarova et al., 2014). Globally, isoprene is predominately emitted from biogenic sources, but anthropogenic sources become increasingly important in urban areas especially, at night (Borbon et al., 2001; Hsieh et al., 2017; Khan et al., 2018a; Mishra and Sinha, 2020; Sahu et al., 2017; Sahu and Saxena, 2015). Monoterpenes are another important BSOA precursor, with annual global emissions estimates of between 89 and 177 $Tg\,yr^{-1}$ (Guenther et al., 2012; Sindelarova et al., 2014). Monoterpenes, while mainly biogenic, are also emitted from anthropogenic sources such as biomass burning, cooking, and fragranced consumer products (Cheng et al., 2018; Gkatzelis et al., 2021; Panopoulou et al., 2020, 2021; Stewart et al., 2021a, c; Zhang et al., 2020).

Numerous studies have identified and quantified molecular-level markers from isoprene and monoterpenes, especially in the south-eastern US and China (Brüggemann et al., 2019; Bryant et al., 2020, 2021; Hettiyadura et al., 2019; Huang et al., 2016; Rattanavaraha et al., 2016; Wang et al., 2016, 2018; Yee et al., 2020). The complex sources of isoprene and monoterpenes in highly polluted urban areas make source identification difficult. As such, the secondary organic aerosol (SOA) markers in this study are referred to as originating from isoprene or monoterpenes, but the emissions are likely from a mixture of biogenic and anthropogenic sources as discussed previously (Cash et al., 2021; Nelson et al., 2021).

Recent studies have started to focus on anthropogenic–biogenic interactions, whereby anthropogenic pollutants such as NO_x and sulfate enhance the formation of biogenically derived SOA species. Increased NO or NO_2 concentrations can lead to higher organonitrate (ON) or nitrooxyorganosulfate (NOS) concentrations through $RO_2 + NO$ or volatile organic compound (VOC)–NO_3 pathways (Morales et al., 2021; Takeuchi and Ng, 2019). Inorganic sulfate formed from the oxidation of SO_2 plays a pivotal role in OS and NOS formation (Bryant et al., 2020; Budisulistior-

ini et al., 2015; Glasius et al., 2018; Hettiyadura et al., 2019; Hoyle et al., 2011; Xu et al., 2015). Sulfate allows the acid-catalysed uptake of gas-phase oxidation products into the particle phase. Both chamber and ambient studies have shown the direct link between sulfate and OS concentrations (Brüggemann et al., 2020b; Bryant et al., 2020; Budisulistiorini et al., 2015; Gaston et al., 2014; Lin et al., 2012; Riva et al., 2019; Surratt et al., 2008; Xu et al., 2015). Yee et al. (2020) highlighted markers from both the high- and low-NO isoprene oxidation pathways correlated linearly with sulfate over a large range of sulfate concentrations (0.01–10 $\mu g\,m^{-3}$) across central Amazonia during the wet and dry seasons and in the SE US summer. They conclude that the majority of isoprene oxidation products in pre-industrial settings are still expected to be in the form of isoprene OS (OSi), suggesting that they cannot be thought of as purely a biogenic–anthropogenic product (Yee et al., 2020).

In this study, offline $PM_{2.5}$ filter samples were collected across two campaigns (pre- and post-monsoon) in central Delhi, alongside a comprehensive suite of gas and aerosol atmospheric pollutant measurements. Filters were analysed using ultra-high-performance liquid chromatography tandem mass spectrometry and isoprene and monoterpene OS and NOS markers identified and quantified. Isoprene and monoterpene emissions were observed to correlate strongly to anthropogenic markers, suggesting mixed anthropogenic/biogenic sources of these VOCs. OSi species showed strong seasonality and strong correlations to particulate sulfate. NOS species showed strong nocturnal enhancements, likely due to nitrate radical chemistry. This study is the first molecular-level particle-phase analysis of OS and NOS markers from isoprene and monoterpenes in Delhi and aims to improve our understanding of the sources of isoprene and monoterpene SOA markers and their formation pathways in extremely polluted urban environments.

2 Experimental

2.1 Filter collection and site information

$PM_{2.5}$ filter samples were collected as part of the Air Pollution and Human Health (APHH)-India campaign, at the Indira Gandhi Delhi Technical University for Women in New Delhi, India, (28°39′55″ N, 77°13′56″ E). The site is situated inside the Third Ring Road, which caters to huge volumes of traffic, with a major road to the east, between the site and the Yamuna River. Two train stations are located to the south and south-west of the site, and there are several green spaces locally in all directions (Nelson et al., 2021; Stewart et al., 2021c). Filters were collected during two field campaigns in 2018. The first campaign was during the pre-monsoon period, with 35 filters collected between 28 May and 5 June 2018. As part of the second campaign during the post-monsoon period, 108 filters were collected between 9 October and 6 November 2018. Quartz filters (Whatman QMA, 10″ × 8″ or 20.32 cm × 25.4 cm) were pre-baked at 550 °C for 5 h and wrapped in foil before use. Samples were collected using a HiVol sampler (Ecotech 3000, Victoria Australia) with a selective $PM_{2.5}$ inlet at a flow rate of 1.33 $m^3\,min^{-1}$. Once collected, filters were stored in foil at −20 °C before, during, and after transport for UK-based analysis.

2.2 Filter extraction

Using a standard square filter cutter, a section of filter was taken with an area of 30.25 cm^2, which was then cut into roughly 1 cm^2 pieces and placed in a 20 mL glass vial. Next, 8 mL of liquid chromatography–mass spectrometry (LC–MS) grade methanol (MeOH; Optima, Fisher Chemical, USA) was added to the sample and sonicated for 45 min. Ice packs were used to keep the bath temperature below room temperature, with the water swapped mid-way through. Using a 5 mL plastic syringe, the MeOH extract was then pushed through a 0.22 µm filter (Millipore) into another sample vial. An additional 2 mL (2 × 1 mL) of MeOH was added to the filter sample and then extracted through the filter to give a combined extract of ∼ 10 mL. This extract was then reduced to dryness using a Genevac solvent evaporator under vacuum. The dry sample was then reconstituted in 50 : 50 MeOH : H_2O (Optima, Fisher Chemical, USA) for analysis (Bryant et al., 2020; Spolnik et al., 2018). Extraction efficiencies of 2-methyl-glyceric acid (2-MG-OS) and camphorsulfonic acid were determined using authentic standards spiked onto a pre-baked clean filter, and recoveries were calculated to be 71 % and 99 %, respectively.

2.3 Ultra-high-performance liquid chromatography tandem mass spectrometry (UHPLC-MS^2)

The extracted fractions of the filter samples were analysed using an Ultimate 3000 UHPLC (Thermo Scientific, USA) coupled to a Q Exactive Orbitrap MS (Thermo Fisher Scientific, USA) using data-dependent tandem mass spectrometry (ddMS^2) with a heated electrospray ionization (HESI) source. The UHPLC method uses a reversed-phase, 5 µm, 4.6 mm × 100 mm, polar end-capped Accucore column (Thermo Scientific, UK) held at 40 °C. The mobile phase consisted of water (A, Optima-grade) and methanol (B, Optima-grade), both with 0.1 % (v/v) of formic acid (98 % purity, Acros Organics). Gradient elution was used, starting at 90 % (A) with a 1 min post-injection hold, decreasing to 10 % (A) at 26 min, returning to the starting mobile-phase conditions at 28 min, followed by a 2 min hold allowing the re-equilibration of the column. The flow rate was set to 0.3 mL min^{-1}. A sample injection volume of 4 µL was used. The capillary and auxiliary gas heater temperatures were set to 320 °C, with a sheath gas flow rate of 45 (arbitrary unit, arb.) and an auxiliary gas flow rate of 20 (arb.). Spectra were acquired in the negative ionization mode with a

scan range of mass-to-charge ratio (m/z) of 50 to 750, with a mass resolution of 140 000. Tandem mass spectrometry was performed using higher-energy collision dissociation with a stepped normalized collision energy of 10, 45, and 60. The isolation window was set to m/z 2.0 with a loop count of 10, selecting the 10 most abundant species for fragmentation in each scan.

A mass spectral library was built using the compound database function in TraceFinder 4.1 General Quan software (Thermo Fisher Scientific, USA). To build the library, compounds from previous studies (Chan et al., 2011; Nestorowicz et al., 2018; Ng et al., 2008; Riva et al., 2016b; Schindelka et al., 2013; Surratt et al., 2008) were searched for in an afternoon and a night-time filter sample extract analysis using the Xcalibur software. Further details can be found in Bryant et al. (2021) and the Supplement. Isoprene OS and NOS markers were quantified using authentic standards of 2-MG-OS and 2-methyl tetrol OS (2-MT-OS), with later-eluting monoterpene OS and NOS quantified using camphorsulfonic acid. Standards were run across a nine-point calibration curve (2 ppm–7.8 ppb, $R^2 > 0.99$). More details about the method can be found in Bryant et al. (2021). Overall uncertainties associated with calibrations, proxy standards, and matrix effects were estimated. The uncertainties associated with 2-MG-OS and 2-MT-OS were calculated to be 58.9 % and 37.6 %, respectively, mainly due to the large uncertainties in the matrix correction factors. Isoprene SOA markers quantified by the average of 2-MT-OS and 2-MG-OS calibrations have an associated uncertainty of 69.9 %. For monoterpene SOA species which were quantified by camphorsulfonic acid, the associated uncertainty is estimated to be 24.8 %.

2.4 Supplementary measurements

A suite of complementary measurements were made alongside the filter collection including VOCs (Stewart et al., 2021c), oxygenated VOCs, NO_x, CO, O_3, SO_2, HONO, photolysis rates, and measurements of PM_1 non-refractory aerosol chemical components with a high-resolution aerosol mass spectrometer (HR-AMS). Detailed instrument descriptions can be found in Nelson et al. (2021). Briefly, VOCs and oxygenated VOCs were measured via two gas chromatography (GC) instruments (DC-GS-FID and GC-GC-FID). NO_x was measured via a dual-channel chemiluminescence analyser fitted with a blue-light converter for NO_2 (Air Quality Designs Inc., Colorado) alongside CO, which was measured with a resonance fluorescent instrument (Model Al5002, Aerolaser GmbH, Germany). O_3 was measured as outlined by Squires et al. (2020) using an ozone analyser (49i, Thermo Scientific). SO_2 was measured using a 43i SO_2 analyser (Thermo Scientific). High-resolution aerosol mass spectrometry measurements were conducted as outlined in Cash et al. (2021). Ion chromatography measurements were undertaken by the experimental approach outlined by Xu et al. (2020) as part of an intercomparison study. Briefly, filter cuttings were taken from the filter and extracted ultrasonically for 30 min in 10 mL of ultrapure water and then filtered before analysis (Xu et al., 2020).

Meteorology data were downloaded from the NOAA Integrated Surface Database via the worldmet R package for the Indira Gandhi International Airport (code: 421810-99999) (Carslaw, 2021). The planetary boundary layer height (PBLH) was obtained from the ERA5 (ECMWF Reanalysis 5) data product at 0.25° resolution in 1 h time steps at the position lat. 28.625°, long. 77.25°. The data for both campaigns were then selected between the start time of the first filter of that campaign and the end time of the last filter of the same campaign.

3 Results

3.1 Meteorology

The time series for temperature, RH, PBLH, and ventilation coefficient (VC) across the pre- and post-monsoon campaigns are shown in Fig. S1. For the pre-monsoon campaign, the average air temperature was (35.8 ± 4.5) °C compared to (24.7 ± 4.6) °C in the post-monsoon campaign (Table S2). The pre-monsoon campaign also showed higher average wind speeds, with an average of (3.8 ± 1.4) m s^{-1}, compared to (1.7 ± 1.3) m s^{-1} in the post-monsoon campaign. The average RHs of the pre- and post-monsoon were (39.4 ± 13.6) % and (57.3 ± 16.6) %, respectively, both showing similar diurnals with a minimum around mid-morning and nocturnal maximum (Fig. S2). The PBLH shows a similar diurnal between the two campaigns, with the nocturnal boundary layer breaking down around 06:00–07:00 IST with a midday peak, before re-establishing the nocturnal boundary layer around 19:00. The pre-monsoon PBLH has an average maximum of ~ 2400 m compared to post-monsoon ~ 1700 m and a minimum of 270 m compared to 52 m (Fig. S2). The ventilation coefficient (VC = wind speed × PBLH) has been used previously to identify periods of adverse meteorological conditions and gives an idea of how stagnant atmospheric conditions are and the general role of the atmosphere in the dilution of species (Gani et al., 2019). As shown in Fig. S1, the conditions during the post-monsoon campaign were much more stagnant than the pre-monsoon campaign. The VC was on average 4.5 times higher during the pre-monsoon campaign compared to the post-monsoon campaign (Table S2), in line with previous studies (Gani et al., 2019; Saha et al., 2019). The more stagnant conditions during the post-monsoon campaign likely trap nocturnal emissions and their reaction products close to the surface, allowing for a significant build-up of concentrations.

3.2 Gas-phase observations

Time series of the observed mixing ratios (ppbv) of NO, NO_2, and O_3 are shown in Fig. 1 for the pre- and post-monsoon campaigns. The campaign-averaged diurnal profiles are shown in Fig. S3, and the mean, median, and maximum mixing ratios are given in Table S2. It should be noted that only 1 week of data was available for the pre-monsoon period. During the post-monsoon campaign, extremely high mixing ratios of NO were observed with a campaign maximum mixing ratio of ~ 870 ppbv during the early morning of 1 November. During the early part of the pre-monsoon campaign, a large enhancement in NO was observed with mixing ratios around 400 ppbv (Fig. S4), followed by significantly lower concentrations throughout the rest of the campaign. The campaign-average NO diurnal profile shows very high NO mixing ratios at night (pre-monsoon: ~ 50 ppbv; post-monsoon: ~ 300 ppbv), with low afternoon mixing ratios < 2 ppbv due to ozone titration. These high NO concentrations at night likely reduce any night-time chemistry through reactions with NO_3 radicals and ozone. NO_2 during the pre-monsoon was observed to increase as the boundary layer reduced in the late afternoon, with a mid-afternoon minimum. During the post-monsoon, a double peak in concentrations was observed, in line with increasing ozone in the morning and increasing NO in the afternoon. Ozone showed a strong diurnal variation across both campaigns, with average afternoon mixing ratios of ~ 75 ppbv and pre- and post-monsoon maximums of 182 and 134 ppbv, respectively. Night-time O_3 concentrations were significantly higher during the pre-monsoon campaign, likely due to the significantly lower NO concentrations.

3.3 Particle-phase observations

The sampling site was heavily polluted in terms of particulate matter. The mean $\pm\sigma$ $PM_{2.5}$ concentration (Table S2) during the pre-monsoon campaign was $(141 \pm 31)\,\mu g\,m^{-3}$ with a spike in concentrations of $672\,\mu g\,m^{-3}$ on 1 June 2018 at 21:00 IST (Fig. 1). The diurnal (Fig. S5) shows concentrations generally flat throughout the day. During the post-monsoon campaign, the average $PM_{2.5}$ concentration was higher at $(182 \pm 94)\,\mu g\,m^{-3}$, with a spike in concentrations of $695\,\mu g\,m^{-3}$ at the end of the campaign (Fig. 1). The diurnal shows a mid-afternoon minimum with high morning and night concentrations. HR-AMS was used to measure the PM_1 sulfate and total organics. Campaign-averaged total organic concentrations were approximately double in the post-monsoon $(48.7 \pm 35.4)\,\mu g\,m^{-3}$ compared to the pre-monsoon $(19.8 \pm 13.7)\,\mu g\,m^{-3}$. During the pre-monsoon campaign, concentrations are generally flat throughout the day, with an increase in the late afternoon, likely as the boundary layer decreases (Fig. S5). During the post-monsoon, a much more prominent diurnal is observed, with a midday minimum and high night-time concentrations. This diurnal is likely driven by boundary layer conditions. Sulfate averaged $(7.5 \pm 1.8)\,\mu g\,m^{-3}$ during the pre-monsoon campaign, with slightly lower average concentrations observed in the post-monsoon: $(5.6 \pm 2.7)\,\mu g\,m^{-3}$, as shown in Fig. S5. The sulfate diurnal variations are similar to those of the organic aerosol.

3.4 Isoprene and monoterpene measurements

Isoprene was measured hourly using gas chromatography with flame ionization detection (GC-FID) across the two campaigns (Nelson et al., 2021), with the time series shown in Fig. 2. The time series highlights similar diurnal variability each day, driven by biogenic emissions. Figure 3 shows the average diurnal profiles of isoprene during pre-monsoon (a) and post-monsoon (b). The mean isoprene mixing ratios were (1.22 ± 1.28) and (0.93 ± 0.65) ppbv, with maximum isoprene mixing ratios of 4.6 and 6.6 ppbv across the pre- and post-monsoon, respectively. This is in the same range as measured in Beijing (winter mean: (1.21 ± 1.03) ppbv; summer mean: (0.56 ± 0.55) ppbv; Acton et al., 2020), Guangzhou (year-round: 1.14 ppbv) (Zou et al., 2019), and Taipei (summer daytime: (1.26) ppbv; autumn daytime: (0.38) ppbv) (Wang et al., 2013). The diurnal variability observed in the pre-monsoon period corresponds to a typical biogenic-emission-driven profile, with a rapid increase in isoprene around 05:00, reaching a peak around or after midday, before a nocturnal minimum. Figure 3 indicates that average daytime peak isoprene mixing ratios during the pre-monsoon campaign were roughly double that of the post-monsoon campaign. In contrast, average nocturnal mixing ratios of isoprene were 5 times higher in the post-monsoon compared to the pre-monsoon $((0.65 \pm 0.43)$ versus (0.13 ± 0.18) ppbv). In the post-monsoon campaign, isoprene mixing ratios show a strong biogenic-emission-driven diurnal profile at the start of the campaign. However, towards the end of the post-monsoon measurement period, the isoprene mixing ratios become less variable, with a high mixing ratio maintained overnight (Fig. 2). This is potentially due to more stagnant conditions, as observed by the VC in Fig. S1.

A recent study in Delhi averaged across post-monsoon, summer, and winter campaigns found that at vegetative sites biogenic isoprene contributed on average 92 %–96 % to the total isoprene, while at traffic-dominated sites only 30 %–39 % of isoprene was from biogenic sources (Kashyap et al., 2019). This is similar to the contributions of biogenic isoprene (40 %) to total isoprene mixing ratios at the traffic-dominated Marylebone Road London site (Khan et al., 2018a). To gain some understanding of the sources of isoprene at our site in Delhi, the observed concentrations of isoprene were correlated to CO, which is an anthropogenic combustion tracer (Fig. 5), similar to previous studies (Khan et al., 2018a; Wagner and Kuttler, 2014). The isoprene concentrations were split between night and day (pre-monsoon night: 19:00–05:00 IST; pre-monsoon day: 05:00–19:00 IST; post-monsoon night: 17:00–06:00 IST; post-monsoon day:

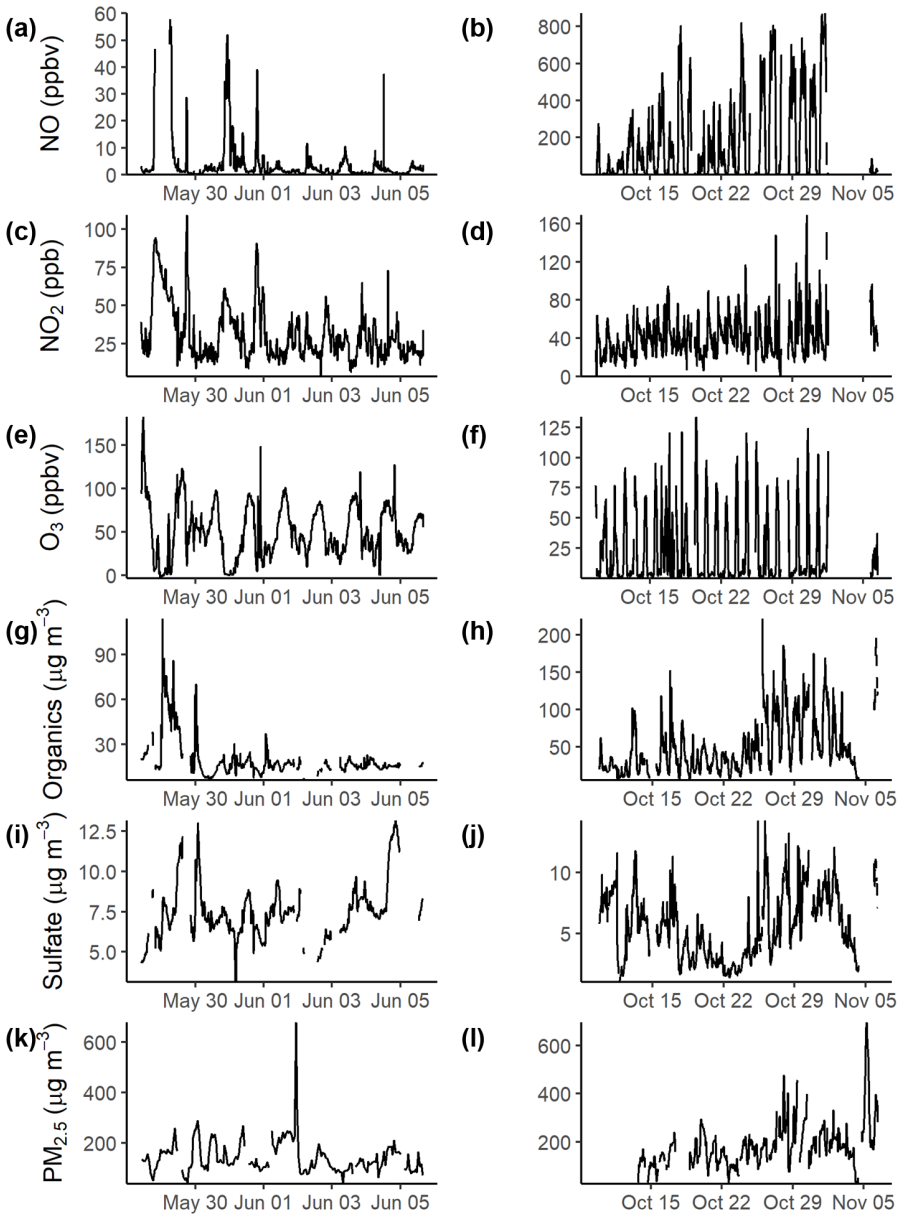

Figure 1. Time series of pollutants across the pre- **(a, c, e, g, i)** and post-monsoon **(b, d, f, h, j)** campaigns. During the pre-monsoon, NO concentrations were filtered to below 60 ppbv, due to a large enhancement in concentrations at the start of the campaign. The full time series is shown in Fig. S4. NO, NO_2, O_3, and HR-AMS–SO_4^{2-} were averaged to 15 min. $PM_{2.5}$ was measured hourly.

06:00–17:00 IST), based on the observed isoprene diurnals as shown in Fig. 3. Isoprene correlated strongly with CO during the night across both campaigns (pre-monsoon: $R^2 = 0.69$; post-monsoon: $R^2 = 0.81$), but no correlation was observed during the day ($R^2 < 0.1$). This suggests that daytime isoprene is predominantly from biogenic sources, although a small amount will be from anthropogenic sources, and that nocturnal isoprene is emitted from anthropogenic sources, as seen in other locations (Khan et al., 2018b; Panopoulou et al., 2020; Wang et al., 2013). The night-time isoprene mixing ratios (pre-monsoon: (0.13 ± 0.18) ppbv; post-monsoon: (0.65 ± 0.43) ppbv) were substantially higher than measured previously in Beijing and London (< 50 pptv; Bryant et al., 2020; Khan et al., 2018b), but pre-monsoon concentrations were similar to those observed at night in Taipei (0.19 ppbv) (Wang et al., 2013). The high night-time concentrations during the post-monsoon period, towards the end of October, are also likely influenced by the formation of a very low boundary layer, trapping pollutants near the surface, affecting all species similarly. An increase in biomass burning may also be a factor. Therefore, during the post-monsoon campaign a

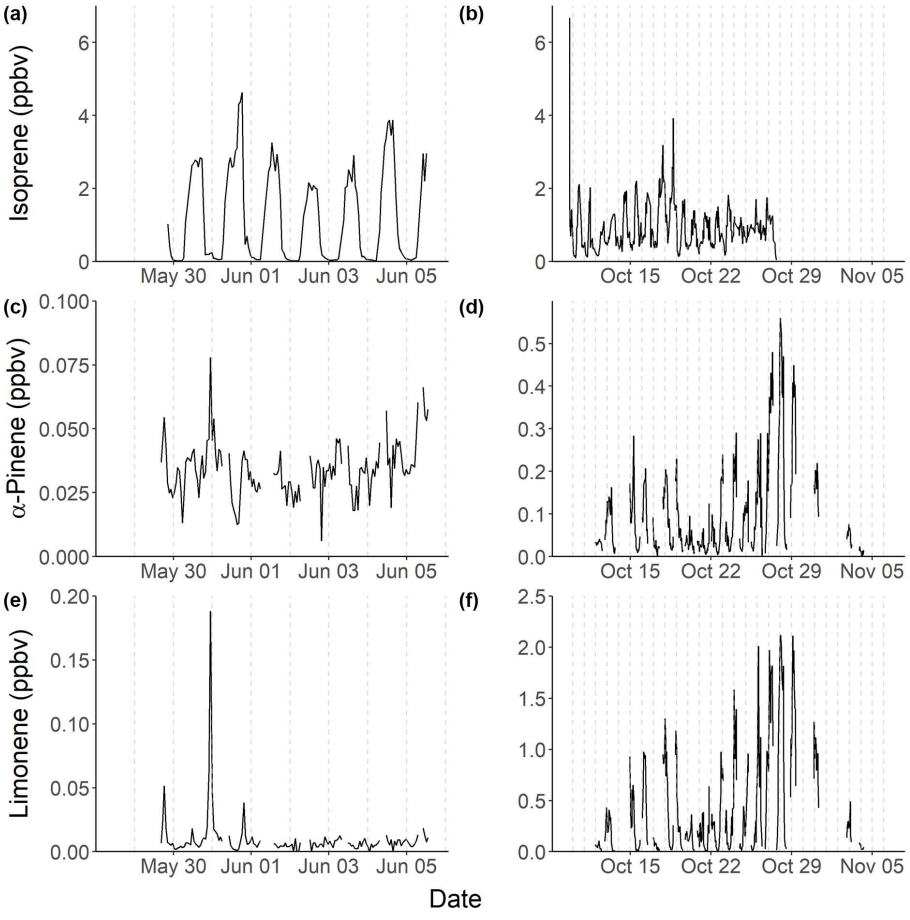

Figure 2. Time series across the pre- **(a, c, e)** and post-monsoon **(b, d, f)** campaigns of isoprene **(a, b)**, α-pinene **(c, d)**, and limonene **(d, e)**. The vertical dotted lines represent midnight for each day.

significant number of isoprene oxidation products will be of anthropogenic origin.

Several monoterpenes were measured using a two-dimensional GC flame ionization detector (GCxGC-FID). The time series of two monoterpenes, limonene and α-pinene, are shown in Fig. 2. The α-pinene mixing ratio averaged (0.034 ± 0.011) ppbv during the pre-monsoon and (0.10 ± 0.11) ppbv during the post-monsoon periods. This is in comparison to limonene, which averaged (0.01 ± 0.02) ppbv and (0.42 ± 0.51) ppbv across the pre- and post-monsoon campaigns, respectively. A strong diurnal variation was observed for both monoterpenes during the post-monsoon, peaking during the night (Fig. 3), with a mid-day minimum. Nocturnal mixing ratios of the two monoterpenes were substantially higher during the post-monsoon (limonene: (0.59 ± 0.11) ppbv; α-pinene: (0.13 ± 0.12) ppbv) than the pre-monsoon (limonene: (0.011 ± 0.025) ppbv; α-pinene: (0.033 ± 0.009) ppbv) period. The diurnal variations across both campaigns are likely driven by both emissions and boundary layer effects. The boundary layer effect however is much stronger during the post-monsoon, with a shallower nocturnal boundary layer; as such the post-monsoon period has a more pronounced diurnal. Limonene was dominated by three short-lived spikes in concentrations towards the start of the campaign (Fig. 2). α-pinene concentrations generally increased during the morning, before decreasing during the afternoon. Multiple monoterpenes were measured concurrently using GCxGC-FID (Nelson et al., 2021; Stewart et al., 2021c). For all MT species, the post-monsoon period had higher mean mixing ratios, with large nocturnal enhancements in mixing ratios. There are likely multiple factors leading the higher concentrations during the post-monsoon, including accumulation due to boundary layer effects, a lack of nocturnal radical chemistry, and an increase in biomass burning (Jain et al., 2014). The average isomeric speciation of the measured monoterpenes showed low variability between daytime and night-time samples during each campaign, but significant differences were observed between the campaigns (Fig. 4). Higher contributions from limonene and β-ocimene were observed during the post-monsoon compared to the pre-monsoon. The reason for the difference in composition is

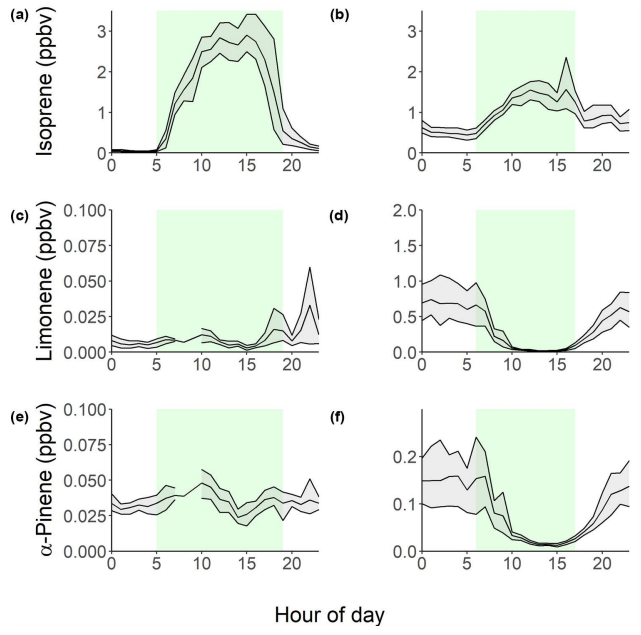

Figure 3. Diurnal variations across the pre- **(a, c, e)** and post-monsoon **(b, d, f)** campaigns of isoprene **(a, b)**, limonene **(c, d)**, and α-pinene **(e, f)**. The shaded grey area represents the 95 % confidence interval. The shaded green area represents the times driven by biogenic emissions, as defined by the isoprene diurnals.

likely due to differences in sources and/or sinks between the two periods.

During the post-monsoon, α-pinene and limonene correlated strongly with CO during the day (α-pinene: $R^2 = 0.82$; limonene: $R^2 = 0.90$) and moderately at night (α-pinene: $R^2 = 0.49$; limonene: $R^2 = 0.56$), as shown in Fig. 5, suggesting anthropogenic sources. Other potentially important anthropogenic monoterpene sources include biomass burning, cooking, and the use of personal care/volatile chemical products (Coggon et al., 2021; Gkatzelis et al., 2021; Hatch et al., 2019; Klein et al., 2016). The shallow nocturnal boundary layers across both campaigns leads to relatively high concentrations of total monoterpenes, with a maximum mixing ratio of 6 ppbv observed during the post-monsoon (Stewart et al., 2021c). After sunrise, the expanding boundary layer dilutes the high concentrations alongside increasing OH concentrations from photolytic sources such as the photolysis of HONO and carbonyls, which likely causes a rapid decrease in the monoterpene mixing ratios (Lelieveld et al., 2016).

3.5 Isoprene and monoterpene OS and NOS formation

At the measured concentrations, monoterpenes and isoprene are an important source of ozone and OH reactivity at this site (Nelson et al., 2021). The resultant oxidized products will also be a key source of SOA production. The UHPLC-MS^2 analysis identified and quantified 75 potential markers across four classes of SOA: isoprene OS (OSi)- and NOS (NOSi)-derived species and monoterpene OS (OS_{MT}) and NOS (NOS_{MT}) species. Figure 6 shows the contribution to the total quantified SOA (qSOA), which consists of the time-averaged sum of the four SOA classes (OSi, NOSi, OS_{MT}, NOS_{MT}), across the pre- and post-monsoon campaigns. OSi species were the dominant SOA class quantified in this study, contributing 75.6 % and 79.4 % of the qSOA across the pre- and post-monsoon campaigns, respectively. NOSi species contributed significantly more to the qSOA during the pre-monsoon (7.6 %) compared to the post-monsoon (2.1 %) period. Similar contributions from the monoterpene-derived SOA species were observed across both campaigns.

3.5.1 Isoprene OS and NOS markers

OSi species are predominantly formed by photo-oxidation of isoprene by OH radicals, with the subsequent products formed dependent on ambient NO concentrations (Wennberg et al., 2018). The pathways are split into high NO and low NO, although the NO concentrations that constitute high and low are a sliding scale depending on the amount of reactivity (defined as $([OH] \times k_{OH})$ (Newland et al., 2021). Under low-NO conditions, isoprene epoxydiol isomers (IEPOX) (Paulot et al., 2009) are formed, which can then undergo reactive uptake to the particle phase by acid-catalysed multiphase chemistry involving inorganic sulfate to form 2-MT-OS (Lin et al., 2012; Riva et al., 2019; Surratt et al., 2010). Under high-NO conditions, 2-methyl glyceric acid is the dominant gas-phase marker produced, which can undergo reactive uptake to the particle phase to form 2-MG-OS (Lin et al., 2013b; Nguyen et al., 2015; Surratt et al., 2006, 2010).

A total of 21 potential OSi C_{2-5} markers previously identified in chamber studies (Nguyen et al., 2010; Riva et al., 2016c; Surratt et al., 2007, 2008) and other ambient studies (Bryant et al., 2020; Budisulistiorini et al., 2015; Hettiyadura et al., 2019; Kourtchev et al., 2016; Rattanavaraha et al., 2016; Wang et al., 2018, 2021b) were quantified in the collected ambient samples. It should be noted that several of the smaller (C_{2-3}) OSi tracers likely form from glyoxal, methylglyoxal, and hydroxyacetone as well as isoprene, and as such present a potential non-isoprene source of OSi (Galloway et al., 2009; Liao et al., 2015).

Figure 6 shows the time series of total OSi concentrations observed across pre-monsoon (left, 5a) and post-monsoon (right, 5b) campaigns. Total OSi time-averaged concentrations (Table 1) were ca. 2.3 times higher during the post-monsoon ($\sim 556.6 \pm 422.5\,ng\,m^{-3}$) campaign than the pre-monsoon campaign ($\sim 237.8 \pm 118.4\,ng\,m^{-3}$). These concentrations are similar to those observed in Beijing during summer 2017 ($237.1\,ng\,m^{-3}$; Bryant et al., 2020) but higher than those observed in Shanghai in 2018 ($40.4\,ng\,m^{-3}$) and 2019 ($34.3\,ng\,m^{-3}$) (Wang et al., 2021b). As previously discussed, OSi species have been shown to form via the gas-phase photo-oxidation of isoprene, with the reactive uptake of the oxidized species into the particulate phase via sulfate

Table 1. Molecular formulae, retention times (RTs), and time-weighted means (ng m^{-3}) of organosulfate (OS) and nitrooxy organosulfate (NOS) species from isoprene (i) and monoterpenes (MTs) observed across pre- and post-monsoon campaigns in Delhi.

Class	Molecular formula	Pre-monsoon	SD	Post-monsoon	SD	RTs (min)
OS_i	$C_5H_{12}O_7S$	38.79	30.19	17.91	19.87	0.71
	$C_5H_{10}O_5S$	26.16	23.30	53.63	131.19	0.93
	$C_2H_4O_6S$	21.35	18.27	84.65	82.79	0.73
	$C_5H_{10}O_6S$	19.80	13.78	45.87	29.47	0.79
	$C_4H_8O_7S$	19.70	12.48	47.96	39.01	0.73
	$C_3H_6O_5S$	19.50	12.47	35.27	40.15	0.73
	$C_5H_8O_7S$	18.76	11.01	38.75	25.34	0.73
	$C_4H_8O_6S$	16.57	9.77	45.48	37.46	0.74
	$C_5H_{10}O_7S$	11.82	7.04	25.89	18.06	0.73
	$C_3H_6O_6S$	6.64	5.00	38.06	40.30	0.73
	$C_4H_8O_5S$	6.46	4.08	22.44	21.39	0.75
	$C_5H_{10}O_8S$	6.25	5.07	7.00	5.54	0.73
	$C_2H_4O_5S$	5.33	3.37	15.92	13.79	0.73
	$C_2H_6O_5S$	5.23	6.36	24.99	20.38	0.73
	$C_5H_8O_5S$	5.16	2.57	7.87	7.93	0.85
	$C_3H_6O_7S$	3.54	3.49	14.78	11.50	0.75
	$C_5H_{12}O_6S$	2.01	1.23	6.53	4.32	0.74
	$C_3H_8O_6S$	1.90	1.08	12.25	10.82	0.75
	$C_5H_8O_9S$	1.20	1.04	2.12	1.85	0.64
	$C_4H_6O_6S$	1.10	0.76	8.61	15.65	0.74
	$C_5H_{12}O_8S$	0.55	0.43	0.65	0.61	0.75
	Total	237.83		556.64		
NOS_i	$C_5H_{10}O_{11}N_2S$	18.65	8.77	11.63	8.09	1.39, 1.92, 2.85, 3.4
	$C_5H_{11}O_9NS$	8.55	5.71	5.93	5.06	0.86
	$C_5H_9O_{10}NS$	3.91	3.46	1.42	1.31	0.94
	$C_5H_{11}O_8NS$	1.52	0.84	1.17	1.20	1.09
	$C_5H_9O_{13}N_3S$	0.002	0.001	0.011	0.009	6.67, 7.89, 8.06
	Total	32.63		20.15		
OS_{MT}	$C_9H_{16}O_6S$	1.10	0.61	1.67	0.88	6.67, 7.14, 7.5, 8.3
	$C_{10}H_{18}O_5S$	0.56	0.63	0.10	0.12	3.39
	$C_{10}H_{16}O_5S$	0.28	0.13	0.77	0.06	4.91, 7, 9.08, 10.9, 11.33, 11.97, 13.26
	$C_{10}H_{20}O_7S$	0.25	0.21	0.27	0.21	4.19
	$C_{10}H_{16}O_7S$	0.23	0.15	0.21	0.13	3.61, 11.68
	$C_9H_{16}O_7S$	0.16	0.17	0.22	0.19	4.39, 6.77
	$C_{10}H_{18}O_6S$	0.15	0.10	NA	NA	10.27
	$C_9H_{14}O_6S$	0.15	1.10	0.25	0.14	3.5, 5.81
	$C_{10}H_{16}O_6S$	0.10	0.06	0.06	0.03	9.33
	$C_{10}H_{18}O_8S$	0.02	0.01	0.04	0.24	7.24
	$C_8H_{14}O_7S$	0.04	0.03	0.10	0.15	4.46
	Total	3.05		3.68		
NOS_{MT}	$C_{10}H_{17}NO_7S$	5.96	3.33	13.36	4.98	9.1, 10.16, 10.67, 10.92, 11.07, 11.36, 11.57, 12.01, 13.28
	$C_9H_{15}NO_8S$	1.12	0.51	2.79	1.14	3.5, 5.81
	$C_{10}H_{17}NO_9S$	0.47	0.19	1.15	0.29	3.93, 5.34, 6.39, 7.89, 9.26, 10.11, 17.94
	$C_9H_{15}NO_9S$	0.0216	0.0044	0.22	0.14	2.69, 3.46
	$C_{10}H_{17}NO_8S$	0.01	0.01	0.07	0.04	5.77
	Total	7.59		17.59		

NA: not available.

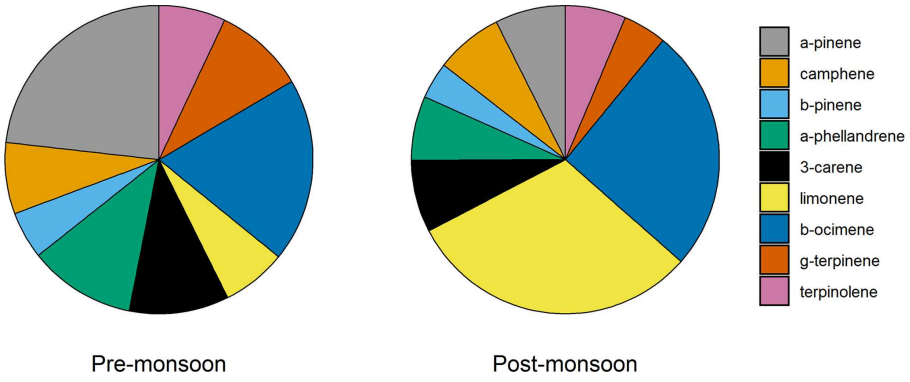

Figure 4. Average composition of monoterpenes across the pre-monsoon and post-monsoon periods.

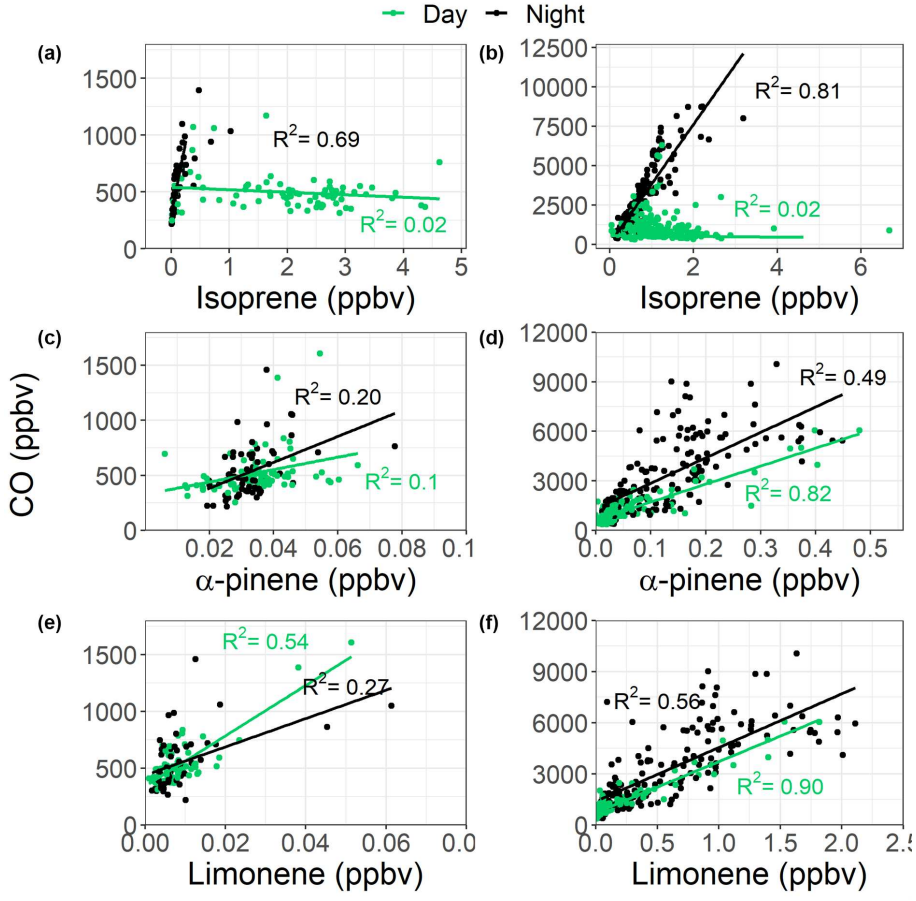

Figure 5. Correlations between isoprene, limonene, and α-pinene with CO across the pre- **(a, c, e)** and post-monsoon **(b, d, f)** campaigns. The samples are split between daytime (green) and night-time (black) as defined by the isoprene diurnals in Fig. 3.

(Lin et al., 2013b; Surratt et al., 2010). Recently, a heterogeneous photo-oxidation pathway from 2-MT-OS ($C_5H_{12}O_7S$) to several OSi species was proposed, including $C_5H_{10}O_7S$, $C_5H_8O_7S$, $C_5H_{12}O_8S$, $C_5H_{10}O_8S$, and $C_4H_8O_7S$ (Chen et al., 2020); 2-MT-OS showed moderate correlations (pre-monsoon: $R^2 = 0.52$–0.72; post-monsoon: $R^2 = 0.14$–0.35) with these OSi tracers that were lower than observed in Beijing summer ($R^2 = 0.83$–0.92) (Bryant et al., 2020). These correlations could suggest that this is a more common formation route in pre-monsoon Delhi than in post-monsoon. However, the correlations could also be driven by the common pathways between the OSi species, with the reactive uptake of gas-phase intermediates via sulfate reactions. The lower correlations during the post-monsoon could be due to

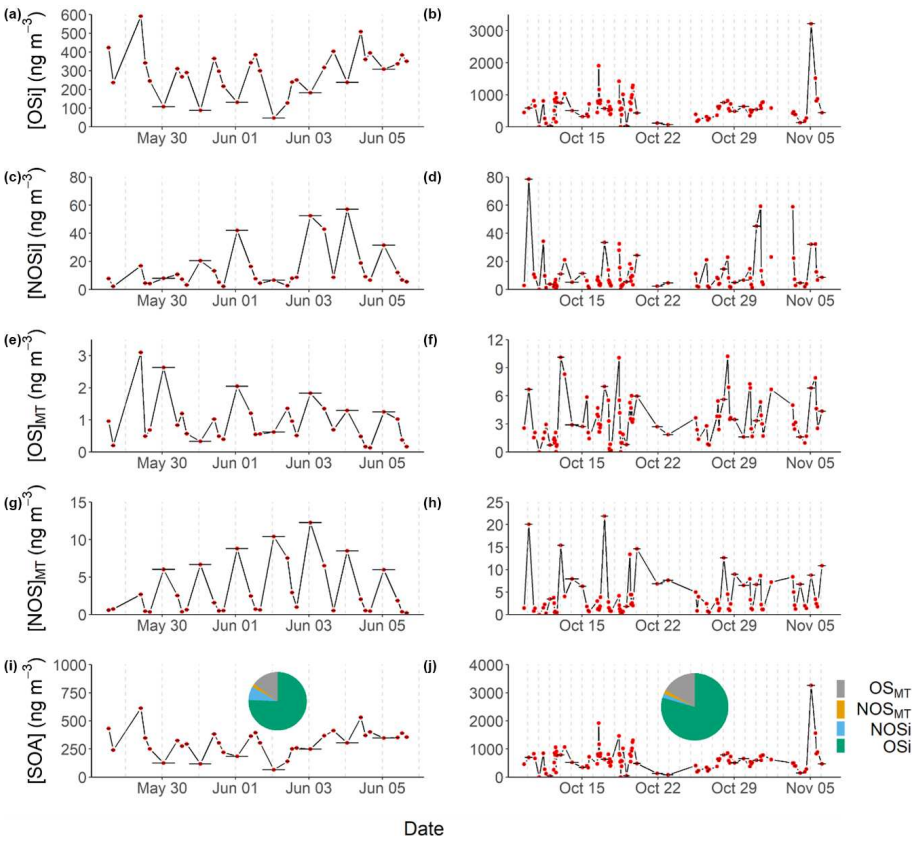

Figure 6. Time series across the pre- **(a, c, e, g, i)** and post-monsoon **(b, d, f, h, j)** campaigns of the quantified SOA tracers: OSi **(a, b)**, NOSi **(c, d)**, OS_{MT} **(e, f)**, NOS_{MT} **(g, h)**, and the sum of all SOA tracers **(i, j)** with the average campaign contributions. The vertical dotted lines represent midnight for each day. Only species identified in more than 40 % of the samples for each campaign were included.

increased influences of anthropogenic sources coupled to the stagnant conditions.

Figure 7 shows the binned OSi concentrations for each filter collection time across the pre- and post-monsoon campaigns to create a partial diurnal profile. During the pre-monsoon, the daily variation in OSi concentrations was much clearer, with daytime maxima and nocturnal minima, which are in line with daily peak isoprene (Fig. 3) and OH radical concentrations. The highest observed OSi concentrations during the pre-monsoon were $\sim 600\,\mathrm{ng\,m^{-3}}$, which occurred at the start of the campaign. High isoprene concentrations may have been the cause, but unfortunately isoprene measurements were not available during this period to confirm. However, high OSi concentrations also occurred when particulate inorganic sulfate concentrations were at their highest (Fig. S6), while sulfate measured via the HR-AMS was also high during this period (Fig. 1). During the post-monsoon, although a similar diurnal pattern was observed, the variation was less pronounced, with higher OSi concentrations observed at the start and end of the campaign (Fig. 6). Due to the secondary nature of sulfate, the sulfate concentrations are less likely to be influenced by the boundary layer effects, compared to directly emitted VOCs. The low OSi concentrations during the middle of the campaign coincide with lower isoprene and inorganic sulfate concentrations, but also low VC values, suggesting more stagnant conditions.

The sum of OSi species across all filters sampled showed a variable correlation with particulate sulfate across both campaigns. The pre-monsoon correlation was similar to those observed in Beijing, Guangzhou, and the SE US (R^2: 0.55) (Bryant et al., 2020, 2021; Budisulistiorini et al., 2015; Rattanavaraha et al., 2016) while the post-monsoon was significantly weaker (R^2: 0.28). However, a clear relationship between OSi tracers and inorganic sulfate can be seen in Fig. 8 across both campaigns, where the highest OSi concentrations occurred under the highest particulate sulfate concentrations. During the post-monsoon campaign, OSi concentrations levelled off at high sulfate concentrations. In the pre-monsoon this levelling-off is not observed, potentially due to the lower number of samples. The high concentrations of organics measured by the HR-AMS (Table S2) during the post-monsoon ($(48.7 \pm 35.4)\,\mu\mathrm{g\,m^{-3}}$) compared to the pre-monsoon ($(19.8 \pm 13.7)\,\mu\mathrm{g\,m^{-3}}$) suggests that the reactive uptake of the gaseous OSi intermediates to the aerosol phase may be limited due to extensive organic coatings on the sulfate aerosol. Multiple studies have now shown that or-

ganic coatings on sulfate aerosol can limit the reactive uptake of IEPOX, suggesting that the pre-monsoon is volume-limited, but the post-monsoon is diffusion-limited (Gaston et al., 2014; Lin et al., 2014; Riva et al., 2016a).

Isoprene NOSs (NOSi's) have been shown to be produced by photo-oxidation in the presence of NO and from NO_3 oxidation chemistry (Hamilton et al., 2021; Ng et al., 2017; Surratt et al., 2008). A total of 10 different NOSi tracers were screened for across the 2 campaigns, with 8 identified in the pre-monsoon and 10 in the post-monsoon. These tracers included mono-nitrated ($C_5H_9O_{10}NS$, $C_5H_{11}O_9NS$, $C_5H_{11}O_8NS$), di-nitrated ($C_5H_{10}O_{11}N_2S$), and tri-nitrated ($C_5H_9O_{13}N_3S$) species. These tracers have been identified previously in China (Bryant et al., 2020, 2021; Hamilton et al., 2021; Wang et al., 2018, 2021b). Unlike the OSi tracers, total NOSi concentrations were on average higher during the pre-monsoon (32.6 ± 19.9) ng m^{-3} compared to the post-monsoon (20.2 ± 13.3) ng m^{-3}. This is likely due to extremely high night-time NO concentrations during the post-monsoon quenching NO_3 radicals, limiting the isoprene–NO_3 pathway. The NOSi time series and diurnal shown in Figs. 5 and 6, respectively, highlight the strong nocturnal enhancements in concentrations during the pre-monsoon, suggesting that the isoprene–NO_3 formation pathway is dominant. Due to the long sampling time, it is likely that these species are forming in the early evening as NO_3 oxidation becomes more competitive with OH, while isoprene concentrations are still relatively high. During the post-monsoon, NOSi concentrations were highest at night and the early morning. The high morning concentrations could be due to non-local sources mixing down as the shallow night-time boundary layer breaks down. Ideally, future work in Delhi or India should focus on the measurements of radicals and OH reactivity (k_{OH}) in order to improve our understanding of the chemistry occurring in extremely polluted environments. A large spike in NOSi concentrations is observed at the start of the post-monsoon campaign, which was not observed for the OS_i tracers; this coincides with lower NO concentrations than the rest of the post-monsoon campaign, reducing the NO_3 quenching by NO, allowing for more isoprene–NO_3 oxidation. The NOSi species did not correlate towards particulate sulfate ($R^2 < 0.2$) across either campaign, suggesting that uptake onto sulfate is not the limiting step in NOSi formation (unlike for the OSi species).

3.5.2 Monoterpene OS and NOS markers

Monoterpene-derived OS (OS_{MT}) and NOS (NOS_{MT}) markers have also been identified from the oxidation by OH, NO_3, and O_3 in the presence of SO_2 or sulfate seed in simulation studies (Brüggemann et al., 2020a; Iinuma et al., 2007; Kleindienst et al., 2006; Surratt et al., 2008; Zhao et al., 2018). Compared to isoprene, the ozonolysis of monoterpenes is a key degradation pathway, with higher SOA yields from ozonolysis observed when compared to isoprene (Jonsson et al., 2005; Atkinson and Arey, 2003; Eddingsaas et al., 2012a, b; Kristensen et al., 2013; Mutzel et al., 2016; Simon et al., 2020; Zhao et al., 2015). A recent study in the SE US suggests that the degradation of 80 % of monoterpenes at night is due to ozonolysis at that location (Zhang et al., 2018). Monoterpene-derived OS and NOS species have been extensively observed, with ON contributing considerably to OA (Lee et al., 2016; Xu et al., 2015; Zhang et al., 2018). Recently NOS hydrolysis has also been shown to be a potential formation route of OS particle-phase species (Darer et al., 2011; Passananti et al., 2016).

Twenty-three monoterpene-derived organosulfate (OS_{MT}) species, which have been seen previously in chamber (Surratt et al., 2008) and ambient studies (Brüggemann et al., 2019; Wang et al., 2018, 2021b), were identified across the pre- and post-monsoon campaigns. It should be noted that recently OS_{MT} artefacts have been shown to form when filters have been sampled without a denuder (Brüggemann et al., 2020a). However, the strong diurnal variations in the OS_{MT} species and lack of correlation with SO_2 suggest this process is unlikely to have contributed significantly to the OS_{MT} measured in this study. Post-monsoon concentrations were similar (3.96 ± 1.6) ng m^{-3} to the pre-monsoon (3.05 ± 1.3) ng m^{-3}, with $C_9H_{16}O_6S$ the dominant species across both campaigns, contributing on average ~ 29 % of the OS_{MT} mass. $C_9H_{16}O_6S$ has been observed in chamber studies (Surratt et al., 2008) as well as in ambient samples in Denmark, Shanghai, and Guangzhou previously (Bryant et al., 2021; Nguyen et al., 2014; Wang et al., 2017). It should be noted that the majority of the OS_{MT} species were not identified in every sample, and as such only tracers which were identified in at least 40 % of the samples were examined further.

Total OS_{MT} showed a strong diurnal profile across both campaigns, peaking at night, with an afternoon minimum (Figs. 5 and 6). During the pre-monsoon campaign, the highest OS_{MT} concentrations were observed during a daytime sample, coinciding with peak sulfate and NO concentrations. Both limonene and α-pinene also show peaks during this filter sampling period of ~ 0.05 ppbv. Spikes in limonene and α-pinene concentrations were also observed on 31 May, but OS_{MT} concentrations were much lower, likely due to the lower sulfate concentrations. During the post-monsoon campaign, nocturnal enhancements are observed (Fig. 7), suggesting $MT - NO_3$ chemistry is important. Like the NOSi markers, higher OS_{MT} concentrations were observed during the early morning sample, likely due to a lower PBLH concentrating the markers coupled to MT–OH and MT–O_3 occurring after sunrise in the post-monsoon. The night-time formation of the OS_{MT} species is in line with previous studies (Bryant et al., 2021) and with the diurnal variations in α-pinene and limonene, which peak at night. Previous chamber studies investigating reactions of monoterpenes with NO_3 radicals have also shown formation of OS_{MT} with the same molecular formulae as measured here (Surratt et al., 2008).

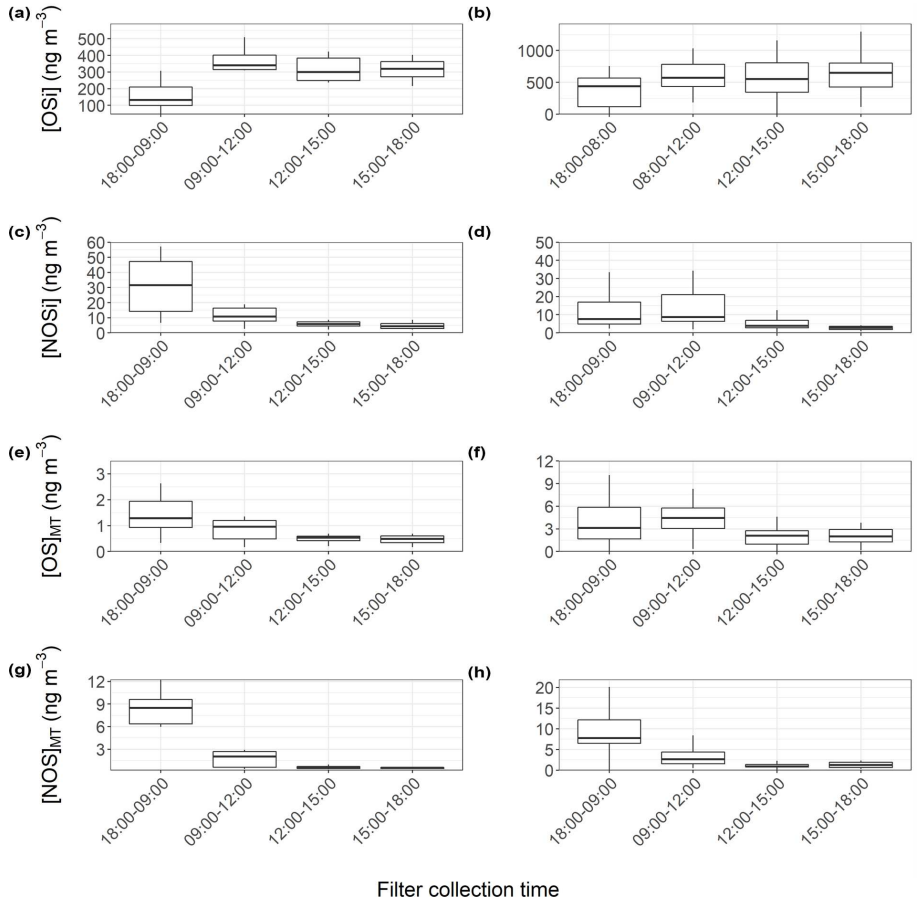

Figure 7. Partial diurnal variations from the binned concentrations of OSi, NOSi, OS_{MT}, and NOS_{MT} concentrations at each filter collection time across the pre- **(a, c, e, g)** and post-monsoon **(b, d, f, h)** campaigns. The lower and upper parts of the box represent the 25th and 75th percentiles, with the upper and lower lines extending no further than 1.5 times the interquartile range of the highest and lowest values within the hinge, respectively. Only species identified in more than 40 % of the samples for each campaign were included.

OS_{MT} concentrations observed in Delhi are much lower than those of the OSi, similar to other studies (Hettiyadura et al., 2019; Wang et al., 2018, 2021b). Considering the high concentrations of extremely reactive α-pinene and limonene observed during the post-monsoon period, higher OS_{MT} concentrations might be expected. One possible reason for the low OS_{MT} is the inability of OS_{MT} precursor species to undergo reactive uptake into the aerosol phase under atmospherically relevant acidic conditions, with chamber studies suggesting extremely acidic conditions are needed for uptake to occur (Drozd et al., 2013). Delhi is characterized by large concentrations of free ammonia and alkaline dust, and previous studies have highlighted that it has less acidic aerosol (pH 5.7–6.7; Kumar et al., 2018) across the year than Beijing (pH 3.8–4.5; Ding et al., 2019) and the SE US (pH 1.6–1.9; Rattanavaraha et al., 2016).

Unlike the OS_{MT} species, the NOS_{MT} species ($C_{10}H_{17}NO_7S$, $C_9H_{15}NO_8S$, $C_{10}H_{17}NO_9S$, $C_9H_{15}NO_9S$, $C_{10}H_{17}NO_8S$) showed strong seasonality, with pre- and post-monsoon concentrations of (7.6 ± 3.8) and

Table 2. Comparison of $C_{10}H_{17}NO_7S$ concentrations across different locations. Locations and concentrations in bold were quantified by authentic standards.

Location	$C_{10}H_{17}NO_7S$ ($ng\,m^{-3}$)	Reference
Delhi Pre-monsoon	5.96	This study
Delhi Post-monsoon	13.36	This study
Guangzhou summer	7.15	Bryant et al. (2021)
Guangzhou winter	11.11	Bryant et al. (2021)
Shanghai 15/16	6.21	Wang et al. (2021b)
Shanghai 16/17	5.55	Wang et al. (2021b)
Beijing	12.00	Wang et al. (2018)
Atlanta	9.00	Hettiyadura et al. (2019)
Hong Kong	**5.61**	**Wang et al. (2021a)**
Guangzhou	**12.32**	**Wang et al. (2021a)**
Shanghai	**16.51**	**Wang et al. (2021a)**
Beijing	**13.15**	**Wang et al. (2021a)**

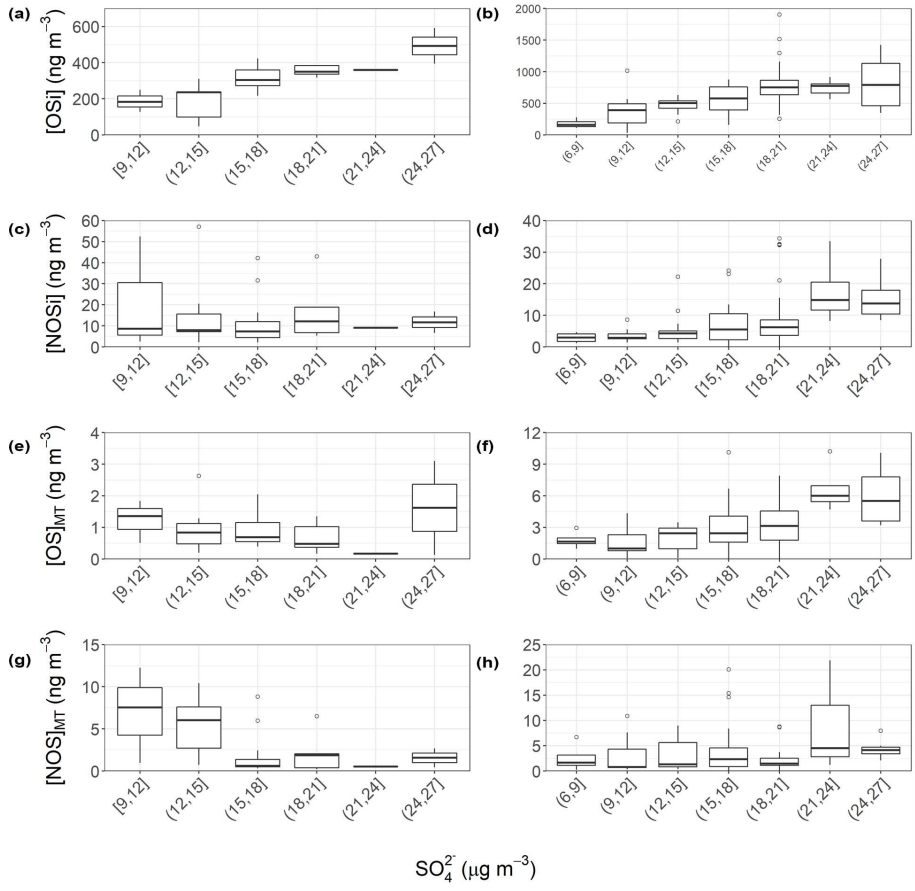

Figure 8. Quantified SOA (OS_i, NOS_i, OS_{MT}, NOS_{MT}) vs. inorganic sulfate concentrations across the pre- **(a, c, e, g)** and post-monsoon **(b, d, f, h)** campaigns. The lower and upper parts of the box represent the 25th and 75th percentiles, with the upper and lower lines extending no further than 1.5 times the interquartile range of the highest and lowest values within the hinge, respectively. Only species identified in more than 40 % of the samples for each campaign were included.

$(17.6 \pm 6.1)\,ng\,m^{-3}$, respectively. This is opposite to the quantified NOSi species, which showed higher pre-monsoon concentrations. This is likely due to much higher post-monsoon concentrations of monoterpenes. Of the NOS_{MT} species observed, $C_{10}H_{17}NO_7S$ was the most abundant, contributing on average 79 % and 76 % of the NOS_{MT} concentrations across the pre- and post-monsoon, respectively. Previous studies have also highlighted that $C_{10}H_{17}NO_7S$ is the dominant monoterpene-derived sulfate-containing tracer (Wang et al., 2018). In the post-monsoon nine $C_{10}H_{17}NO_7S$ isomers were observed, and seven were observed in the pre-monsoon. The summed $C_{10}H_{17}NO_7S$ concentrations during the pre- $((5.96 \pm 3.33)\,ng\,m^{-3})$ and post-monsoon $((13.36 \pm 4.98)\,ng\,m^{-3})$ are of a similar magnitude to those observed in other locations, as shown in Table 2. These concentrations are also similar to those quantified by authentic standards across four Chinese megacities (Wang et al., 2021a). Like the OS_{MT} species, some NOS_{MT} species were not identified in many of the filter samples, and as such tracers which were observed in more than 40 % of the samples were summed for further analysis. The NOS_{MT} pre-monsoon time series (Fig. 6) shows a similar temporal profile to the NOSi species, with lower concentrations during the enhancement in NO concentrations (Fig. S4) at the start of the campaign. NOS_{MT} showed strong diurnal variations across both campaigns (Fig. 7), peaking at night, with lower concentrations during the afternoon, as seen previously (Bryant et al., 2021; Wang et al., 2018). Therefore, the formation of NOS_{MT} is likely dominated by NO_3 radical chemistry. Both NOS_{MT} and OS_{MT} species showed limited correlation towards SO_2 and particulate sulfate ($R^2 < 0.1$), indicating that although sulfate is essential to their formation, sulfate availability does not control NOS_{MT} concentrations.

3.5.3 Contributions of total isoprene and monoterpene OS and NOS (qSOA) to particulate mass

Particulate concentrations in Delhi are among the highest across the world (World's most polluted cities (historical data 2017–2021): https://www.iqair.com/in-en/

world-most-polluted-cities, last access: 22 December 2022), with concentrations over 600 $\mu g\,m^{-3}$ being observed during this study; qSOA, defined here as the sum of all OSi, NOSi, OS_{MT}, and NOS_{MT} tracers quantified (including those not identified in more than 40 % of the samples), was calculated to determine the total contribution these species make to particulate mass in Delhi. Total oxidized organic aerosol (OOA), a proxy for SOA in PM_1, was derived from the HR-AMS measurements during the pre- and post-monsoon campaigns, with averages of (19.8 ± 13.7) and $(48.7 \pm 35.4)\,\mu g\,m^{-3}$, respectively; qSOA contributed on average (2.0 ± 0.9) % and (1.8 ± 1.4) % to the total OOA. Isoprene- and monoterpene-derived species contributed on average 83.2 % and 16.8 % of qSOA across the pre-monsoon, respectively, compared to 81.5 % and 18.5 % during the post-monsoon, respectively. During certain periods qSOA contributed a maximum of 4.2 % and 6.6 % to OOA during the pre- and post-monsoon, respectively. This is under the assumption that when the OS and NOS species fragment in the AMS ion source they lose their sulfate and nitrate groups. This is similar to the contributions made by OSi markers in Beijing to total OOA (2.2 %) (Bryant et al., 2020). Previous studies in the SE US have reported much higher contributions of isoprene species to total OA. As quantified by an aerosol chemical speciation monitor, summed isoprene SOA tracers on average accounted for 9.4 % of measured OA at Look Rock, downwind of Maryville and Knoxville, but up to a maximum of 28.1 % (Budisulistiorini et al., 2015). This is lower than that measured at a rural site at Yorkville, Georgia, with just low-NO isoprene SOA tracers accounting for between 12 %–19 % of total OA (Lin et al., 2013a).

Sulfate was also measured in the PM_1 size range by HR-AMS, with pre- and post-monsoon mean concentrations of (7.5 ± 1.8) and $(5.5 \pm 2.7)\,\mu g\,m^{-3}$. The sulfate-containing OS and NOS species quantified in this study may fragment in the AMS to produce a sulfate signal which is not related to inorganic sulfate. To estimate the contribution that sulfate contained within qSOA species could make to total AMS sulfate, the quantified mass of sulfate contained within each marker was calculated based on the fraction of sulfate to each marker of molecular mass. For example, 2-MT-OS has an accurate mass of m/z 216.21, meaning the percentage of 2-MT-OS mass associated with sulfate is ~ 44 %. During the pre-monsoon campaign the qSOA sulfate accounted for on average 2.2 % of the total PM_1 sulfate, but up to 4.8 % on certain days; qSOA contributed considerably more to the sulfate in the post-monsoon campaign, with an average of (6.1 ± 4.5) % and a maximum of 18.7 %. This finding indicates the need to consider the sources of particulate sulfate measured by the AMS when calculating aerosol pH. The sulfate contribution from the fragmentation of common small OS compounds (hydroxymethanesulfonate, methanesulfonic acid) can be distinguished in the AMS using the relative ratio of sulfur-containing fragments (Chen et al., 2019). However, more work is needed to determine how larger OS and NOS fragment in the AMS such as those quantified in this study. Overall, this highlights that isoprene and MT oxidation can make significant contributions to organic and sulfate-containing aerosol, even in extremely polluted environments such as Delhi. It should be noted that this is just a subset of potentially many more SOAs from isoprene and monoterpene markers and only focusses on sulfate-containing species.

4 Conclusion

Isoprene- and monoterpene-derived organosulfate (OS) and nitrooxy organosulfate (NOS) species were quantified during pre- and post-monsoon measurement periods in the Indian megacity of Delhi. An extensive dataset of supplementary measurements was obtained alongside filter samples, including isoprene and speciated monoterpenes. Isoprene and monoterpene emissions were found to be highly influenced by anthropogenic sources, with strong correlations to anthropogenic tracers at night across both campaigns. High nocturnal concentrations of pollutants were observed due to a low boundary layer height and stagnant conditions, especially during the post-monsoon period.

Isoprene OS markers (OSi) were observed in higher concentrations during the post-monsoon ($(557 \pm 423)\,ng\,m^{-3}$) compared to the pre-monsoon campaign ($(238 \pm 118)\,ng\,m^{-3}$). OSi showed a moderate correlation with inorganic sulfate across both campaigns. However, concentrations levelled off at high sulfate concentrations during the post-monsoon, which is consistent with organic coatings limiting uptake of isoprene epoxides. Isoprene NOS species (NOSi) showed nocturnal enhancements across both campaigns, while the highest average concentrations were observed in the morning samples of the post-monsoon campaign. The high morning concentrations are likely due to the oxidation of VOCs by OH radicals from photolytic processes throughout the morning. Monoterpene-derived OS (OS_{MT}) and NOS (NOS_{MT}) markers were observed to have nocturnal enhancements in concentrations, in line with their precursors. NOS_{MT} markers were observed in similar concentrations to those of other megacities. Total quantified SOA contributed on average (2.0 ± 0.9) % and (1.8 ± 1.4) % to the total OOA. Considering high OOA concentrations were observed across the two campaigns, the total markers contributed up to a maximum of 4.2 % and 6.6 % across the pre- and post-monsoon, respectively. Overall, this work highlights that even small numbers of isoprene- and monoterpene-derived SOA markers can make significant contributions to OA mass, even in highly polluted megacities.

Data availability. Data used in this study can be accessed from the CEDA archive: https://catalogue.ceda.ac.uk/uuid/

ba27c1c6a03b450e9269f668566658ec (last access: May 2022; Nemitz et al., 2020).

Supplement. The supplement related to this article is available online at: https://doi.org/10.5194/acp-23-61-2023-supplement.

Author contributions. DJB prepared the manuscript with contributions from all authors. DJB, BSN, SJS, SHB, WSD, ARV, JMC, WJFA, BL, EN, and JRH provided measurements and data processing of pollutants used in this study. MJN and ARR contributed to scientific discussion. S, RG, BRG, TM, and EN assisted with logistics. CNH, JDL, ARR, and JFH provided overall guidance to the experimental set-up and design.

Competing interests. The contact author has declared that none of the authors has any competing interests.

Disclaimer. Publisher's note: Copernicus Publications remains neutral with regard to jurisdictional claims in published maps and institutional affiliations.

Acknowledgements. The authors acknowledge Tuhin Mandal at CSIR National Physical Laboratory for his support in facilitating the measurement sites used in this project and Gareth Stewart for the VOC measurements. This work was supported by the Newton Bhabha fund administered by the UK Natural Environment Research Council through the DelhiFlux and ASAP projects of the Atmospheric Pollution and Human Health in an Indian Megacity (APHH-India) programme. The authors gratefully acknowledge the financial support provided by the UK Natural Environment Research Council and the Earth System Science Organization, Ministry of Earth Sciences, Government of India, under the Indo-UK Joint Collaboration (DelhiFlux). Daniel J. Bryant and Beth S. Nelson acknowledge the NERC SPHERES doctoral training programme for studentships. James M. Cash is supported by a NERC E3 DTP studentship.

Financial support. This research has been supported by the Natural Environment Research Council (grant nos. NE/P016502/1 and NE/P01643X/1) and the Government of India, Ministry of Earth Sciences (DelhiFlux (grant no. MoES/16/19/2017/APHH)).

Review statement. This paper was edited by Ivan Kourtchev and reviewed by two anonymous referees.

References

Acton, W. J. F., Huang, Z., Davison, B., Drysdale, W. S., Fu, P., Hollaway, M., Langford, B., Lee, J., Liu, Y., Metzger, S., Mullinger, N., Nemitz, E., Reeves, C. E., Squires, F. A., Vaughan, A. R., Wang, X., Wang, Z., Wild, O., Zhang, Q., Zhang, Y., and Hewitt, C. N.: Surface–atmosphere fluxes of volatile organic compounds in Beijing, Atmos. Chem. Phys., 20, 15101–15125, https://doi.org/10.5194/acp-20-15101-2020, 2020.

Anand, V., Korhale, N., Rathod, A., and Beig, G.: On processes controlling fine particulate matters in four Indian megacities, Environ. Pollut., 254, 113026, https://doi.org/10.1016/j.envpol.2019.113026, 2019.

Atkinson, R. and Arey, J.: Gas-phase tropospheric chemistry of biogenic volatile organic compounds: A review, Atmos. Environ., 37, 197–219, https://doi.org/10.1016/S1352-2310(03)00391-1, 2003.

Balakrishnan, K., Dey, S., Gupta, T., Dhaliwal, R. S., Brauer, M., Cohen, A. J., Stanaway, J. D., Beig, G., Joshi, T. K., Aggarwal, A. N., Sabde, Y., Sadhu, H., Frostad, J., Causey, K., Godwin, W., Shukla, D. K., Kumar, G. A., Varghese, C. M., Muraleedharan, P., Agrawal, A., Anjana, R. M., Bhansali, A., Bhardwaj, D., Burkart, K., Cercy, K., Chakma, J. K., Chowdhury, S., Christopher, D. J., Dutta, E., Furtado, M., Ghosh, S., Ghoshal, A. G., Glenn, S. D., Guleria, R., Gupta, R., Jeemon, P., Kant, R., Kant, S., Kaur, T., Koul, P. A., Krish, V., Krishna, B., Larson, S. L., Madhipatla, K., Mahesh, P. A., Mohan, V., Mukhopadhyay, S., Mutreja, P., Naik, N., Nair, S., Nguyen, G., Odell, C. M., Pandian, J. D., Prabhakaran, D., Prabhakaran, P., Roy, A., Salvi, S., Sambandam, S., Saraf, D., Sharma, M., Shrivastava, A., Singh, V., Tandon, N., Thomas, N. J., Torre, A., Xavier, D., Yadav, G., Singh, S., Shekhar, C., Vos, T., Dandona, R., Reddy, K. S., Lim, S. S., Murray, C. J. L., Venkatesh, S., and Dandona, L.: The impact of air pollution on deaths, disease burden, and life expectancy across the states of India: the Global Burden of Disease Study 2017, Lancet Planet. Heal., 3, e26–e39, https://doi.org/10.1016/S2542-5196(18)30261-4, 2019.

Bhandari, S., Gani, S., Patel, K., Wang, D. S., Soni, P., Arub, Z., Habib, G., Apte, J. S., and Hildebrandt Ruiz, L.: Sources and atmospheric dynamics of organic aerosol in New Delhi, India: insights from receptor modeling, Atmos. Chem. Phys., 20, 735–752, https://doi.org/10.5194/acp-20-735-2020, 2020.

Borbon, A., Fontaine, H., Veillerot, M., Locoge, N., Galloo, J. C., and Guillermo, R.: An investigation into the traffic-related fraction of isoprene at an urban location, Atmos. Environ., 35, 3749–3760, https://doi.org/10.1016/S1352-2310(01)00170-4, 2001.

Brüggemann, M., van Pinxteren, D., Wang, Y., Yu, J. Z., and Herrmann, H.: Quantification of known and unknown terpenoid organosulfates in PM_{10} using untargeted LC–HRMS/MS: contrasting summertime rural Germany and the North China Plain, Environ. Chem., 16, 333, https://doi.org/10.1071/EN19089, 2019.

Brüggemann, M., Riva, M., Perrier, S., Poulain, L., George, C., and Herrmann, H.: Overestimation of Monoterpene Organosulfate Abundance in Aerosol Particles by Sampling in the Presence of SO_2, Environ. Sci. Technol. Lett., 8, 206–211, https://doi.org/10.1021/acs.estlett.0c00814, 2020a.

Brüggemann, M., Xu, R., Tilgner, A., Kwong, K. C., Mutzel, A., Poon, H. Y., Otto, T., Schaefer, T., Poulain, L., Chan, M. N., and Herrmann, H.: Organosulfates in Ambient Aerosol: State of Knowledge and Future Research Directions on Formation, Abundance, Fate, and Importance, Environ. Sci. Technol., 54, 3767–3782, https://doi.org/10.1021/acs.est.9b06751, 2020b.

Bryant, D. J., Dixon, W. J., Hopkins, J. R., Dunmore, R. E., Pereira, K. L., Shaw, M., Squires, F. A., Bannan, T. J., Mehra, A., Worrall, S. D., Bacak, A., Coe, H., Percival, C. J., Whalley, L. K., Heard, D. E., Slater, E. J., Ouyang, B., Cui, T., Surratt, J. D., Liu, D., Shi, Z., Harrison, R., Sun, Y., Xu, W., Lewis, A. C., Lee, J. D., Rickard, A. R., and Hamilton, J. F.: Strong anthropogenic control of secondary organic aerosol formation from isoprene in Beijing, Atmos. Chem. Phys., 20, 7531–7552, https://doi.org/10.5194/acp-20-7531-2020, 2020.

Bryant, D. J., Elzein, A., Newland, M., White, E., Swift, S., Watkins, A., Deng, W., Song, W., Wang, S., Zhang, Y., Wang, X., Rickard, A. R., and Hamilton, J. F.: Importance of Oxidants and Temperature in the Formation of Biogenic Organosulfates and Nitrooxy Organosulfates, ACS Earth Sp. Chem., 5, acsearthspacechem.1c00204, https://doi.org/10.1021/ACSEARTHSPACECHEM.1C00204, 2021.

Budisulistiorini, S. H., Li, X., Bairai, S. T., Renfro, J., Liu, Y., Liu, Y. J., McKinney, K. A., Martin, S. T., McNeill, V. F., Pye, H. O. T., Nenes, A., Neff, M. E., Stone, E. A., Mueller, S., Knote, C., Shaw, S. L., Zhang, Z., Gold, A., and Surratt, J. D.: Examining the effects of anthropogenic emissions on isoprene-derived secondary organic aerosol formation during the 2013 Southern Oxidant and Aerosol Study (SOAS) at the Look Rock, Tennessee ground site, Atmos. Chem. Phys., 15, 8871–8888, https://doi.org/10.5194/acp-15-8871-2015, 2015.

Carslaw, D.: Access surface meteorological data from the NOAA Integrated Surface Database from around the world, GitHub [code], https://davidcarslaw.github.io/worldmet/reference/worldmet.html, last access: October 2021.

Cash, J. M., Langford, B., Di Marco, C., Mullinger, N. J., Allan, J., Reyes-Villegas, E., Joshi, R., Heal, M. R., Acton, W. J. F., Hewitt, C. N., Misztal, P. K., Drysdale, W., Mandal, T. K., Shivani, Gadi, R., Gurjar, B. R., and Nemitz, E.: Seasonal analysis of submicron aerosol in Old Delhi using high-resolution aerosol mass spectrometry: chemical characterisation, source apportionment and new marker identification, Atmos. Chem. Phys., 21, 10133–10158, https://doi.org/10.5194/acp-21-10133-2021, 2021.

Chan, M. N., Surratt, J. D., Chan, A. W. H., Schilling, K., Offenberg, J. H., Lewandowski, M., Edney, E. O., Kleindienst, T. E., Jaoui, M., Edgerton, E. S., Tanner, R. L., Shaw, S. L., Zheng, M., Knipping, E. M., and Seinfeld, J. H.: Influence of aerosol acidity on the chemical composition of secondary organic aerosol from β-caryophyllene, Atmos. Chem. Phys., 11, 1735–1751, https://doi.org/10.5194/acp-11-1735-2011, 2011.

Chen, Y., Xu, L., Humphry, T., Hettiyadura, A. P. S., Ovadnevaite, J., Huang, S., Poulain, L., Schroder, J. C., Campuzano-Jost, P., Jimenez, J. L., Herrmann, H., O'Dowd, C., Stone, E. A. and Ng, N. L.: Response of the Aerodyne Aerosol Mass Spectrometer to Inorganic Sulfates and Organosulfur Compounds: Applications in Field and Laboratory Measurements, Environ. Sci. Technol., 53, 5176–5186, https://doi.org/10.1021/acs.est.9b00884, 2019.

Chen, Y., Zhang, Y., Lambe, T. A., Xu, R., Lei, Z., Olson, E. N., Zhang, Z., Szalkowski, T., Cui, T., Vizuete, W., Gold, A., Turpin, J. B., Ault, P. A., Nin Chan, M., and Surratt, D. J.: Heterogeneous Hydroxyl Radical Oxidation of Isoprene Epoxydiol-Derived Methyltetrol Sulfates: Plausible Formation Mechanisms of Previously Unexplained Organosulfates in Ambient Fine Aerosols, Environ. Sci.-Technol. Lett., 7, 460–468, https://doi.org/10.1021/acs.estlett.0c00276, 2020.

Cheng, X., Li, H., Zhang, Y., Li, Y., Zhang, W., Wang, X., Bi, F., Zhang, H., Gao, J., Chai, F., Lun, X., Chen, Y. and Lv, J.: Atmospheric isoprene and monoterpenes in a typical urban area of Beijing: Pollution characterization, chemical reactivity and source identification, J. Environ. Sci., 71, 150–167, https://doi.org/10.1016/J.JES.2017.12.017, 2018.

Chowdhury, Z., Zheng, M., Cass, G. R., Sheesley, R. J., Schauer, J. J., Salmon, L. G., and Russell, A. G.: Source apportionment and characterization of ambient fine particles in Delhi, in: Symposium on Air Quality Measurement Methods and Technology 2004, pp. 13–24, 2004.

Coggon, M. M., Gkatzelis, G. I., McDonald, B. C., and Warneke, C.: Volatile chemical product emissions enhance ozone and modulate urban chemistry, P. Natl. Acad. Sci. USA, 118, e2026653118, https://doi.org/10.1073/pnas.2026653118, 2021.

Darer, A. I., Cole-Filipiak, N. C., O'Connor, A. E., and Elrod, M. J.: Formation and stability of atmospherically relevant isoprene-derived organosulfates and organonitrates, Environ. Sci. Technol., 45, 1895–1902, https://doi.org/10.1021/es103797z, 2011.

Ding, J., Zhao, P., Su, J., Dong, Q., Du, X., and Zhang, Y.: Aerosol pH and its driving factors in Beijing, Atmos. Chem. Phys., 19, 7939–7954, https://doi.org/10.5194/acp-19-7939-2019, 2019.

Drozd, G. T., Woo, J. L., and McNeill, V. F.: Self-limited uptake of a-pinene oxide to acidic aerosol: the effects of liquid–liquid phase separation and implications for the formation of secondary organic aerosol and organosulfates from epoxides, Atmos. Chem. Phys., 13, 8255–8263, https://doi.org/10.5194/acp-13-8255-2013, 2013.

Du, Z., He, K., Cheng, Y., Duan, F., Ma, Y., Liu, J., Zhang, X., Zheng, M., and Weber, R.: A yearlong study of water-soluble organic carbon in Beijing I: Sources and its primary vs. secondary nature, Atmos. Environ., 92, 514–521, https://doi.org/10.1016/j.atmosenv.2014.04.060, 2014.

Eddingsaas, N. C., Loza, C. L., Yee, L. D., Chan, M., Schilling, K. A., Chhabra, P. S., Seinfeld, J. H., and Wennberg, P. O.: α-pinene photooxidation under controlled chemical conditions – Part 2: SOA yield and composition in low- and high-NO_x environments, Atmos. Chem. Phys., 12, 7413–7427, https://doi.org/10.5194/acp-12-7413-2012, 2012a.

Eddingsaas, N. C., Loza, C. L., Yee, L. D., Seinfeld, J. H., and Wennberg, P. O.: α-pinene photooxidation under controlled chemical conditions – Part 1: Gas-phase composition in low- and high-NO_x environments, Atmos. Chem. Phys., 12, 6489–6504, https://doi.org/10.5194/acp-12-6489-2012, 2012b.

Elser, M., Huang, R.-J., Wolf, R., Slowik, J. G., Wang, Q., Canonaco, F., Li, G., Bozzetti, C., Daellenbach, K. R., Huang, Y., Zhang, R., Li, Z., Cao, J., Baltensperger, U., El-Haddad, I., and Prévôt, A. S. H.: New insights into $PM_{2.5}$ chemical composition and sources in two major cities in China during extreme haze events using aerosol mass spectrometry, Atmos. Chem. Phys., 16, 3207–3225, https://doi.org/10.5194/acp-16-3207-2016, 2016.

Elzein, A., Stewart, G. J., Swift, S. J., Nelson, B. S., Crilley, L. R., Alam, M. S., Reyes-Villegas, E., Gadi, R., Harrison, R. M., Hamilton, J. F., and Lewis, A. C.: A comparison of $PM_{2.5}$-bound polycyclic aromatic hydrocarbons in summer Beijing (China) and Delhi (India), Atmos. Chem. Phys., 20, 14303–14319, https://doi.org/10.5194/acp-20-14303-2020, 2020.

Galloway, M. M., Chhabra, P. S., Chan, A. W. H., Surratt, J. D., Flagan, R. C., Seinfeld, J. H., and Keutsch, F. N.: Glyoxal uptake on ammonium sulphate seed aerosol: reaction products and reversibility of uptake under dark and irradiated conditions, Atmos. Chem. Phys., 9, 3331–3345, https://doi.org/10.5194/acp-9-3331-2009, 2009.

Gani, S., Bhandari, S., Seraj, S., Wang, D. S., Patel, K., Soni, P., Arub, Z., Habib, G., Hildebrandt Ruiz, L., and Apte, J. S.: Submicron aerosol composition in the world's most polluted megacity: the Delhi Aerosol Supersite study, Atmos. Chem. Phys., 19, 6843–6859, https://doi.org/10.5194/acp-19-6843-2019, 2019.

Gaston, C. J., Riedel, T. P., Zhang, Z., Gold, A., Surratt, J. D., and Thornton, J. A.: Reactive Uptake of an Isoprene-Derived Epoxydiol to Submicron Aerosol Particles, Environ. Sci. Technol., 48, 11178–11186, https://doi.org/10.1021/es5034266, 2014.

Gkatzelis, G. I., Coggon, M. M., McDonald, B. C., Peischl, J., Gilman, J. B., Aikin, K. C., Robinson, M. A., Canonaco, F., Prevot, A. S. H., Trainer, M., and Warneke, C.: Observations Confirm that Volatile Chemical Products Are a Major Source of Petrochemical Emissions in U.S. Cities, Environ. Sci. Technol., 55, 4332–4343, https://doi.org/10.1021/acs.est.0c05471, 2021.

Glasius, M., Bering, M. S., Yee, L. D., de Sá, S. S., Isaacman-VanWertz, G., Wernis, R. A., Barbosa, H. M. J., Alexander, M. L., Palm, B. B., Hu, W., Campuzano-Jost, P., Day, D. A., Jimenez, J. L., Shrivastava, M., Martin, S. T., and Goldstein, A. H.: Organosulfates in aerosols downwind of an urban region in central Amazon, Environ. Sci. Process. Impacts, 20, 1546–1558, https://doi.org/10.1039/C8EM00413G, 2018.

Guenther, A. B., Jiang, X., Heald, C. L., Sakulyanontvittaya, T., Duhl, T., Emmons, L. K., and Wang, X.: The Model of Emissions of Gases and Aerosols from Nature version 2.1 (MEGAN2.1): an extended and updated framework for modeling biogenic emissions, Geosci. Model Dev., 5, 1471–1492, https://doi.org/10.5194/gmd-5-1471-2012, 2012.

Hallquist, M., Wenger, J. C., Baltensperger, U., Rudich, Y., Simpson, D., Claeys, M., Dommen, J., Donahue, N. M., George, C., Goldstein, A. H., Hamilton, J. F., Herrmann, H., Hoffmann, T., Iinuma, Y., Jang, M., Jenkin, M. E., Jimenez, J. L., Kiendler-Scharr, A., Maenhaut, W., McFiggans, G., Mentel, Th. F., Monod, A., Prévôt, A. S. H., Seinfeld, J. H., Surratt, J. D., Szmigielski, R., and Wildt, J.: The formation, properties and impact of secondary organic aerosol: current and emerging issues, Atmos. Chem. Phys., 9, 5155–5236, https://doi.org/10.5194/acp-9-5155-2009, 2009.

Hama, S. M. L., Kumar, P., Harrison, R. M., Bloss, W. J., Khare, M., Mishra, S., Namdeo, A., Sokhi, R., Goodman, P., and Sharma, C.: Four-year assessment of ambient particulate matter and trace gases in the Delhi-NCR region of India, Sustain. Cities Soc., 54, 102003, https://doi.org/10.1016/j.scs.2019.102003, 2020.

Hamilton, J. F., Bryant, D. J., Edwards, P. M., Ouyang, B., Bannan, T. J., Mehra, A., Mayhew, A. W., Hopkins, J. R., Dunmore, R. E., Squires, F. A., Lee, J. D., Newland, M. J., Worrall, S. D., Bacak, A., Coe, H., Whalley, L. K., Heard, D. E., Slater, E. J., Jones, R. L., Cui, T., Surratt, J. D., Reeves, C. E., Mills, G. P., Grimmond, S., Sun, Y., Xu, W., Shi, Z., and Rickard, A. R.: Key Role of NO_3 Radicals in the Production of Isoprene Nitrates and Nitrooxyorganosulfates in Beijing, Environ. Sci. Technol., 55, 842–853, https://doi.org/10.1021/acs.est.0c05689, 2021.

Hatch, L. E., Jen, C. N., Kreisberg, N. M., Selimovic, V., Yokelson, R. J., Stamatis, C., York, R. A., Foster, D., Stephens, S. L., Goldstein, A. H., and Barsanti, K. C.: Highly Speciated Measurements of Terpenoids Emitted from Laboratory and Mixed-Conifer Forest Prescribed Fires, Environ. Sci. Technol., 53, 9418–9428, https://doi.org/10.1021/ACS.EST.9B02612, 2019.

Hettiyadura, A. P. S., Al-Naiema, I. M., Hughes, D. D., Fang, T., and Stone, E. A.: Organosulfates in Atlanta, Georgia: anthropogenic influences on biogenic secondary organic aerosol formation, Atmos. Chem. Phys., 19, 3191–3206, https://doi.org/10.5194/acp-19-3191-2019, 2019.

Hoffmann, T., Odum, J. R., Bowman, F., Collins, D., Klockow, D., Flagan, R. C., and Seinfeld, J. H.: Formation of organic aerosols from the oxidation of biogenic hydrocarbons, J. Atmos. Chem., 26, 189–222, https://doi.org/10.1023/A:1005734301837, 1997.

Hoyle, C. R., Boy, M., Donahue, N. M., Fry, J. L., Glasius, M., Guenther, A., Hallar, A. G., Huff Hartz, K., Petters, M. D., Petäjä, T., Rosenoern, T., and Sullivan, A. P.: A review of the anthropogenic influence on biogenic secondary organic aerosol, Atmos. Chem. Phys., 11, 321–343, https://doi.org/10.5194/acp-11-321-2011, 2011.

Hsieh, H.-C., Ou-Yang, C.-F., and Wang, J.-L.: Revelation of Coupling Biogenic with Anthropogenic Isoprene by Highly Time-Resolved Observations, Aerosol Air Qual. Res., 17, 721–729, https://doi.org/10.4209/AAQR.2016.04.0133, 2017.

Hu, W., Hu, M., Hu, W., Jimenez, J. L., Yuan, B., Chen, W., Wang, M., Wu, Y., Chen, C., Wang, Z., Peng, J., Zeng, L., and Shao, M.: Chemical composition, sources, and aging process of submicron aerosols in Beijing: Contrast between summer and winter, J. Geophys. Res.-Atmos., 121, 1955–1977, https://doi.org/10.1002/2015JD024020, 2016.

Huang, Z., Zhang, Y., Yan, Q., Zhang, Z., and Wang, X.: Real-time monitoring of respiratory absorption factors of volatile organic compounds in ambient air by proton transfer reaction time-of-flight mass spectrometry, J. Hazard. Mater., 320, 547–555, https://doi.org/10.1016/J.JHAZMAT.2016.08.064, 2016.

Iinuma, Y., Müller, C., Berndt, T., Böge, O., Claeys, M., and Herrmann, H.: Evidence for the existence of organosulfates from β-pinene ozonolysis in ambient secondary organic aerosol, Environ. Sci. Technol., 41, 6678–6683, https://doi.org/10.1021/es070938t, 2007.

Jain, N., Bhatia, A., and Pathak, H.: Emission of Air Pollutants from Crop Residue Burning in India, Aerosol Air Qual. Res., 14, 422–430, https://doi.org/10.4209/aaqr.2013.01.0031, 2014.

Jonsson, Å. M., Hallquist, M., and Ljungström, E.: Impact of Humidity on the Ozone Initiated Oxidation of Limonene, Δ3-Carene, and α-Pinene, Environ. Sci. Technol., 40, 188–194, https://doi.org/10.1021/ES051163W, 2005.

Kanawade, V. P., Srivastava, A. K., Ram, K., Asmi, E., Vakkari, V., Soni, V. K., Varaprasad, V., and Sarangi, C.: What caused severe air pollution episode of November 2016 in New Delhi?, Atmos. Environ., 23, 12095–12123, https://doi.org/10.1016/j.atmosenv.2019.117125, 2020.

Kashyap, P., Kumar, A., Kumar, R. P., and Kumar, K.: Biogenic and anthropogenic isoprene emissions in the subtropical urban atmosphere of Delhi, Atmos. Pollut. Res., 10, 1691–1698, https://doi.org/10.1016/j.apr.2019.07.004, 2019.

Khan, M. A. H., Schlich, B.-L., Jenkin, M. E., Shallcross, B. M. A., Moseley, K., Walker, C., Morris, W. C., Derwent, R. G., Percival,

C. J., and Shallcross, D. E.: A Two-Decade Anthropogenic and Biogenic Isoprene Emissions Study in a London Urban Background and a London Urban Traffic Site, Atmosphere, 9, 387, https://doi.org/10.3390/ATMOS9100387, 2018a.

Khan, M. A. H., Schlich, B. L., Jenkin, M. E., Shallcross, B. M. A., Moseley, K., Walker, C., Morris, W. C., Derwent, R. G., Percival, C. J., and Shallcross, D. E.: A Two-Decade Anthropogenic and Biogenic Isoprene Emissions Study in a London Urban Background and a London Urban Traffic Site, Atmosphere, 9, 387, https://doi.org/10.3390/ATMOS9100387, 2018b.

Kirillova, E. N., Sheesley, R. J., Andersson, A., and Gustafsson, Ö.: Natural abundance ^{13}C and ^{14}C analysis of water-soluble organic carbon in atmospheric aerosols, Anal. Chem., 82, 7973–7978, https://doi.org/10.1021/ac1014436, 2010.

Kirillova, E. N., Andersson, A., Sheesley, R. J., Kruså, M., Praveen, P. S., Budhavant, K., Safai, P. D., Rao, P. S. P., and Gustafsson, Ö.: ^{13} C- and ^{14} C-based study of sources and atmospheric processing of water-soluble organic carbon (WSOC) in South Asian aerosols, J. Geophys. Res.-Atmos., 118, 614–626, https://doi.org/10.1002/jgrd.50130, 2013.

Kirillova, E. N., Andersson, A., Tiwari, S., Srivastava, A. K., Bisht, D. S., and Gustafsson, Ö.: Water-soluble organic carbon aerosols during a full New Delhi winter: Isotope-based source apportionment and optical properties, J. Geophys. Res.-Atmos., 119, 3476–3485, https://doi.org/10.1002/2013JD020041, 2014.

Klein, F., Farren, N. J., Bozzetti, C., Daellenbach, K. R., Kilic, D., Kumar, N. K., Pieber, S. M., Slowik, J. G., Tuthill, R. N., Hamilton, J. F., Baltensperger, U., Prévôt, A. S. H., and El Haddad, I.: Indoor terpene emissions from cooking with herbs and pepper and their secondary organic aerosol production potential, Sci. Rep.-UK, 6, 1–7, https://doi.org/10.1038/srep36623, 2016.

Kleindienst, T. E., Edney, E. O., Lewandowski, M., Offenberg, J. H., and Jaoui, M.: Secondary Organic Carbon and Aerosol Yields from the Irradiations of Isoprene and α-Pinene in the Presence of NO_x and SO $_2$, Environ. Sci. Technol., 40, 3807–3812, https://doi.org/10.1021/es052446r, 2006.

Kourtchev, I., Godoi, R. H. M., Connors, S., Levine, J. G., Archibald, A. T., Godoi, A. F. L., Paralovo, S. L., Barbosa, C. G. G., Souza, R. A. F., Manzi, A. O., Seco, R., Sjostedt, S., Park, J.-H., Guenther, A., Kim, S., Smith, J., Martin, S. T., and Kalberer, M.: Molecular composition of organic aerosols in central Amazonia: an ultra-high-resolution mass spectrometry study, Atmos. Chem. Phys., 16, 11899–11913, https://doi.org/10.5194/acp-16-11899-2016, 2016.

Kristensen, K., Enggrob, K. L., King, S. M., Worton, D. R., Platt, S. M., Mortensen, R., Rosenoern, T., Surratt, J. D., Bilde, M., Goldstein, A. H., and Glasius, M.: Formation and occurrence of dimer esters of pinene oxidation products in atmospheric aerosols, Atmos. Chem. Phys., 13, 3763–3776, https://doi.org/10.5194/acp-13-3763-2013, 2013.

Kumar, P., Kumar, S., and Yadav, S.: Seasonal variations in size distribution, water-soluble ions, and carbon content of size-segregated aerosols over New Delhi, Environ. Sci. Pollut. Res., 25, 6061–6078, https://doi.org/10.1007/S11356-017-0954-6, 2018.

Landrigan, P. J., Fuller, R., Acosta, N. J. R., Adeyi, O., Arnold, R., Basu, N. (Nil), Baldé, A. B., Bertollini, R., Bose-O'Reilly, S., Boufford, J. I., Breysse, P. N., Chiles, T., Mahidol, C., Coll-Seck, A. M., Cropper, M. L., Fobil, J., Fuster, V., Greenstone, M., Haines, A., Hanrahan, D., Hunter, D., Khare, M., Krupnick, A., Lanphear, B., Lohani, B., Martin, K., Mathiasen, K. V, McTeer, M. A., Murray, C. J. L., Ndahimananjara, J. D., Perera, F., Potočnik, J., Preker, A. S., Ramesh, J., Rockström, J., Salinas, C., Samson, L. D., Sandilya, K., Sly, P. D., Smith, K. R., Steiner, A., Stewart, R. B., Suk, W. A., van Schayck, O. C. P., Yadama, G. N., Yumkella, K., and Zhong, M.: The Lancet Commission on pollution and health, Lancet, 391, 462–512, https://doi.org/10.1016/S0140-6736(17)32345-0, 2018.

Lanz, V. A., Prévôt, A. S. H., Alfarra, M. R., Weimer, S., Mohr, C., DeCarlo, P. F., Gianini, M. F. D., Hueglin, C., Schneider, J., Favez, O., D'Anna, B., George, C., and Baltensperger, U.: Characterization of aerosol chemical composition with aerosol mass spectrometry in Central Europe: an overview, Atmos. Chem. Phys., 10, 10453–10471, https://doi.org/10.5194/acp-10-10453-2010, 2010.

Lee, B. H., Mohr, C., Lopez-Hilfiker, F. D., Lutz, A., Hallquist, M., Lee, L., Romer, P., Cohen, R. C., Iyer, S., Kurtén, T., Hu, W., Day, D. A., Campuzano-Jost, P., Jimenez, J. L., Xu, L., Ng, N. L., Guo, H., Weber, R. J., Wild, R. J., Brown, S. S., Koss, A., de Gouw, J., Olson, K., Goldstein, A. H., Seco, R., Kim, S., McAvey, K., Shepson, P. B., Starn, T., Baumann, K., Edgerton, E. S., Liu, J., Shilling, J. E., Miller, D. O., Brune, W., Schobesberger, S., D'Ambro, E. L., and Thornton, J. A.: Highly functionalized organic nitrates in the southeast United States: Contribution to secondary organic aerosol and reactive nitrogen budgets, P. Natl. Acad. Sci. USA, 113, 1516–1521, https://doi.org/10.1073/pnas.1508108113, 2016.

Lelieveld, J., Gromov, S., Pozzer, A., and Taraborrelli, D.: Global tropospheric hydroxyl distribution, budget and reactivity, Atmos. Chem. Phys., 16, 12477–12493, https://doi.org/10.5194/acp-16-12477-2016, 2016.

Liao, J., Froyd, K. D., Murphy, D. M., Keutsch, F. N., Yu, G., Wennberg, P. O., St. Clair, J. M., Crounse, J. D., Wisthaler, A., Mikoviny, T., Jimenez, J. L., Campuzano-Jost, P., Day, D. A., Hu, W., Ryerson, T. B., Pollack, I. B., Peischl, J., Anderson, B. E., Ziemba, L. D., Blake, D. R., Meinardi, S., and Diskin, G.: Airborne measurements of organosulfates over the continental U.S., J. Geophys. Res., 120, 2990–3005, https://doi.org/10.1002/2014JD022378, 2015.

Lin, Y. H., Zhang, Z., Docherty, K. S., Zhang, H., Budisulistiorini, S. H., Rubitschun, C. L., Shaw, S. L., Knipping, E. M., Edgerton, E. S., Kleindienst, T. E., Gold, A., and Surratt, J. D.: Isoprene epoxydiols as precursors to secondary organic aerosol formation: Acid-catalyzed reactive uptake studies with authentic compounds, Environ. Sci. Technol., 46, 250–258, https://doi.org/10.1021/es202554c, 2012.

Lin, Y.-H., Knipping, E. M., Edgerton, E. S., Shaw, S. L., and Surratt, J. D.: Investigating the influences of SO_2 and NH_3 levels on isoprene-derived secondary organic aerosol formation using conditional sampling approaches, Atmos. Chem. Phys., 13, 8457–8470, https://doi.org/10.5194/acp-13-8457-2013, 2013a.

Lin, Y. H., Zhang, H., Pye, H. O. T., Zhang, Z., Marth, W. J., Park, S., Arashiro, M., Cui, T., Budisulistiorini, S. H., Sexton, K. G., Vizuete, W., Xie, Y., Luecken, D. J., Piletic, I. R., Edney, E. O., Bartolotti, L. J., Gold, A., and Surratt, J. D.: Epoxide as a precursor to secondary organic aerosol formation from isoprene photooxidation in the presence of ni-

trogen oxides, P. Natl. Acad. Sci. USA, 110, 6718–6723, https://doi.org/10.1073/pnas.1221150110, 2013b.

Lin, Y. H., Budisulistiorini, S. H., Chu, K., Siejack, R. A., Zhang, H., Riva, M., Zhang, Z., Gold, A., Kautzman, K. E., and Surratt, J. D.: Light-absorbing oligomer formation in secondary organic aerosol from reactive uptake of isoprene epoxydiols, Environ. Sci. Technol., 48, 12012–12021, https://doi.org/10.1021/es503142b, 2014.

Mishra, A. K. and Sinha, V.: Emission drivers and variability of ambient isoprene, formaldehyde and acetaldehyde in north-west India during monsoon season, Environ. Pollut., 267, 115538, https://doi.org/10.1016/J.ENVPOL.2020.115538, 2020.

Miyazaki, Y., Aggarwal, S. G., Singh, K., Gupta, P. K., and Kawamura, K.: Dicarboxylic acids and water-soluble organic carbon in aerosols in New Delhi, India, in winter: Characteristics and formation processes, J. Geophys. Res.-Atmos., 114, D19, https://doi.org/10.1029/2009JD011790, 2009.

Morales, A. C., Jayarathne, T., Slade, J. H., Laskin, A., and Shepson, P. B.: The production and hydrolysis of organic nitrates from OH radical oxidation of β-ocimene, Atmos. Chem. Phys., 21, 129–145, https://doi.org/10.5194/acp-21-129-2021, 2021.

Mutzel, A., Rodigast, M., Iinuma, Y., Böge, O., and Herrmann, H.: Monoterpene SOA – Contribution of first-generation oxidation products to formation and chemical composition, Atmos. Environ., 130, 136–144, https://doi.org/10.1016/j.atmosenv.2015.10.080, 2016.

Nagar, P. K., Singh, D., Sharma, M., Kumar, A., Aneja, V. P., George, M. P., Agarwal, N., and Shukla, S. P.: Characterization of $PM_{2.5}$ in Delhi: role and impact of secondary aerosol, burning of biomass, and municipal solid waste and crustal matter, Environ. Sci. Pollut. Res., 24, 25179–25189, https://doi.org/10.1007/s11356-017-0171-3, 2017.

Nelson, B. S., Stewart, G. J., Drysdale, W. S., Newland, M. J., Vaughan, A. R., Dunmore, R. E., Edwards, P. M., Lewis, A. C., Hamilton, J. F., Acton, W. J., Hewitt, C. N., Crilley, L. R., Alam, M. S., Sahin, Ü. A., Beddows, D. C. S., Bloss, W. J., Slater, E., Whalley, L. K., Heard, D. E., Cash, J. M., Langford, B., Nemitz, E., Sommariva, R., Cox, S., Shivani, Gadi, R., Gurjar, B. R., Hopkins, J. R., Rickard, A. R., and Lee, J. D.: In situ ozone production is highly sensitive to volatile organic compounds in Delhi, India, Atmos. Chem. Phys., 21, 13609–13630, https://doi.org/10.5194/acp-21-13609-2021, 2021.

Nemitz, E., Acton, W. J., Alam, M. S., Drysdale, W. S., Dunmore, R. E., Hamilton, J. F., Hopkins, J. R., Langford, B., Nelson, B. S., Stewart, G. S., Vaughan, A. R., and Whalley, L. K.: (APHH India) Megacity Delhi atmospheric emission quantification, assessment and impacts (DelhiFlux), CEDA Archive [data set], https://catalogue.ceda.ac.uk/uuid/ba27c1c6a03b450e9269f668566658ec (last access: May 2022), 2020.

Nestorowicz, K., Jaoui, M., Rudzinski, K. J., Lewandowski, M., Kleindienst, T. E., Spólnik, G., Danikiewicz, W., and Szmigielski, R.: Chemical composition of isoprene SOA under acidic and non-acidic conditions: effect of relative humidity, Atmos. Chem. Phys., 18, 18101–18121, https://doi.org/10.5194/acp-18-18101-2018, 2018.

Newland, M. J., Bryant, D. J., Dunmore, R. E., Bannan, T. J., Acton, W. J. F., Langford, B., Hopkins, J. R., Squires, F. A., Dixon, W., Drysdale, W. S., Ivatt, P. D., Evans, M. J., Edwards, P. M., Whalley, L. K., Heard, D. E., Slater, E. J., Woodward-Massey, R., Ye, C., Mehra, A., Worrall, S. D., Bacak, A., Coe, H., Percival, C. J., Hewitt, C. N., Lee, J. D., Cui, T., Surratt, J. D., Wang, X., Lewis, A. C., Rickard, A. R., and Hamilton, J. F.: Low-NO atmospheric oxidation pathways in a polluted megacity, Atmos. Chem. Phys., 21, 1613–1625, https://doi.org/10.5194/acp-21-1613-2021, 2021.

Ng, N. L., Kwan, A. J., Surratt, J. D., Chan, A. W. H., Chhabra, P. S., Sorooshian, A., Pye, H. O. T., Crounse, J. D., Wennberg, P. O., Flagan, R. C., and Seinfeld, J. H.: Secondary organic aerosol (SOA) formation from reaction of isoprene with nitrate radicals (NO_3), Atmos. Chem. Phys., 8, 4117–4140, https://doi.org/10.5194/acp-8-4117-2008, 2008.

Ng, N. L., Brown, S. S., Archibald, A. T., Atlas, E., Cohen, R. C., Crowley, J. N., Day, D. A., Donahue, N. M., Fry, J. L., Fuchs, H., Griffin, R. J., Guzman, M. I., Herrmann, H., Hodzic, A., Iinuma, Y., Jimenez, J. L., Kiendler-Scharr, A., Lee, B. H., Luecken, D. J., Mao, J., McLaren, R., Mutzel, A., Osthoff, H. D., Ouyang, B., Picquet-Varrault, B., Platt, U., Pye, H. O. T., Rudich, Y., Schwantes, R. H., Shiraiwa, M., Stutz, J., Thornton, J. A., Tilgner, A., Williams, B. J., and Zaveri, R. A.: Nitrate radicals and biogenic volatile organic compounds: oxidation, mechanisms, and organic aerosol, Atmos. Chem. Phys., 17, 2103–2162, https://doi.org/10.5194/acp-17-2103-2017, 2017.

Nguyen, Q. T., Christensen, M. K., Cozzi, F., Zare, A., Hansen, A. M. K., Kristensen, K., Tulinius, T. E., Madsen, H. H., Christensen, J. H., Brandt, J., Massling, A., Nøjgaard, J. K., and Glasius, M.: Understanding the anthropogenic influence on formation of biogenic secondary organic aerosols in Denmark via analysis of organosulfates and related oxidation products, Atmos. Chem. Phys., 14, 8961–8981, https://doi.org/10.5194/acp-14-8961-2014, 2014.

Nguyen, T. B., Bateman, A. P., Bones, D. L., Nizkorodov, S. A., Laskin, J., and Laskin, A.: High-resolution mass spectrometry analysis of secondary organic aerosol generated by ozonolysis of isoprene, Atmos. Environ., 44, 1032–1042, https://doi.org/10.1016/J.ATMOSENV.2009.12.019, 2010.

Nguyen, T. B., Bates, K. H., Crounse, J. D., Schwantes, R. H., Zhang, X., Kjaergaard, H. G., Surratt, J. D., Lin, P., Laskin, A., Seinfeld, J. H., and Wennberg, P. O.: Mechanism of the hydroxyl radical oxidation of methacryloyl peroxynitrate (MPAN) and its pathway toward secondary organic aerosol formation in the atmosphere, Phys. Chem. Chem. Phys., 17, 17914–17926, https://doi.org/10.1039/c5cp02001h, 2015.

Panopoulou, A., Liakakou, E., Sauvage, S., Gros, V., Locoge, N., Stavroulas, I., Bonsang, B., Gerasopoulos, E., and Mihalopoulos, N.: Yearlong measurements of monoterpenes and isoprene in a Mediterranean city (Athens): Natural vs anthropogenic origin, Atmos. Environ., 243, 117803, https://doi.org/10.1016/J.ATMOSENV.2020.117803, 2020.

Panopoulou, A., Liakakou, E., Sauvage, S., Gros, V., Locoge, N., Bonsang, B., Salameh, T., Gerasopoulos, E., and Mihalopoulos, N.: Variability and sources of non-methane hydrocarbons at a Mediterranean urban atmosphere: The role of biomass burning and traffic emissions, Sci. Total Environ., 800, 149389, https://doi.org/10.1016/J.SCITOTENV.2021.149389, 2021.

Passananti, M., Kong, L., Shang, J., Dupart, Y., Perrier, S., Chen, J., Donaldson, D. J., and George, C.: Organosulfate Formation through the Heterogeneous Reaction of

Sulfur Dioxide with Unsaturated Fatty Acids and Long-Chain Alkenes, Angew. Chemie-Int. Ed., 55, 10336–10339, https://doi.org/10.1002/anie.201605266, 2016.

Paulot, F., Crounse, J. D., Kjaergaard, H. G., Kurten, A., St. Clair, J. M., Seinfeld, J. H., and Wennberg, P. O.: Unexpected Epoxide Formation in the Gas-Phase Photooxidation of Isoprene, Science, 325, 730–733, https://doi.org/10.1126/science.1172910, 2009.

Rattanavaraha, W., Chu, K., Budisulistiorini, S. H., Riva, M., Lin, Y.-H., Edgerton, E. S., Baumann, K., Shaw, S. L., Guo, H., King, L., Weber, R. J., Neff, M. E., Stone, E. A., Offenberg, J. H., Zhang, Z., Gold, A., and Surratt, J. D.: Assessing the impact of anthropogenic pollution on isoprene-derived secondary organic aerosol formation in $PM_{2.5}$ collected from the Birmingham, Alabama, ground site during the 2013 Southern Oxidant and Aerosol Study, Atmos. Chem. Phys., 16, 4897–4914, https://doi.org/10.5194/acp-16-4897-2016, 2016.

Reyes-Villegas, E., Panda, U., Darbyshire, E., Cash, J. M., Joshi, R., Langford, B., Di Marco, C. F., Mullinger, N. J., Alam, M. S., Crilley, L. R., Rooney, D. J., Acton, W. J. F., Drysdale, W., Nemitz, E., Flynn, M., Voliotis, A., McFiggans, G., Coe, H., Lee, J., Hewitt, C. N., Heal, M. R., Gunthe, S. S., Mandal, T. K., Gurjar, B. R., Shivani, Gadi, R., Singh, S., Soni, V., and Allan, J. D.: PM_1 composition and source apportionment at two sites in Delhi, India, across multiple seasons, Atmos. Chem. Phys., 21, 11655–11667, https://doi.org/10.5194/acp-21-11655-2021, 2021.

Riva, M., Bell, D. M., Hansen, A. M. K., Drozd, G. T., Zhang, Z., Gold, A., Imre, D., Surratt, J. D., Glasius, M., and Zelenyuk, A.: Effect of Organic Coatings, Humidity and Aerosol Acidity on Multiphase Chemistry of Isoprene Epoxydiols, Environ. Sci. Technol., 50, 5580–5588, https://doi.org/10.1021/acs.est.5b06050, 2016a.

Riva, M., Budisulistiorini, S. H., Zhang, Z., and Gold, A.: Chemical characterization of secondary organic aerosol constituents from isoprene ozonolysis in the presence of acidic aerosol, Atmos. Environ., 130, 5–13, https://doi.org/10.1016/J.ATMOSENV.2015.06.027, 2016b.

Riva, M., Da Silva Barbosa, T., Lin, Y.-H., Stone, E. A., Gold, A., and Surratt, J. D.: Chemical characterization of organosulfates in secondary organic aerosol derived from the photooxidation of alkanes, Atmos. Chem. Phys., 16, 11001–11018, https://doi.org/10.5194/acp-16-11001-2016, 2016c.

Riva, M., Chen, Y., Zhang, Y., Lei, Z., Olson, N. E., Boyer, H. C., Narayan, S., Yee, L. D., Green, H. S., Cui, T., Zhang, Z., Baumann, K., Fort, M., Edgerton, E., Budisulistiorini, S. H., Rose, C. A., Ribeiro, I. O., e Oliveira, R. L., dos Santos, E. O., Machado, C. M. D., Szopa, S., Zhao, Y., Alves, E. G., de Sá, S. S., Hu, W., Knipping, E. M., Shaw, S. L., Duvoisin Junior, S., de Souza, R. A. F., Palm, B. B., Jimenez, J.-L., Glasius, M., Goldstein, A. H., Pye, H. O. T., Gold, A., Turpin, B. J., Vizuete, W., Martin, S. T., Thornton, J. A., Dutcher, C. S., Ault, A. P., and Surratt, J. D.: Increasing Isoprene Epoxydiol-to-Inorganic Sulfate Aerosol Ratio Results in Extensive Conversion of Inorganic Sulfate to Organosulfur Forms: Implications for Aerosol Physicochemical Properties, Environ. Sci. Technol., 53, acs.est.9b01019, https://doi.org/10.1021/acs.est.9b01019, 2019.

Saha, D., Soni, K., Mohanan, M. N., and Singh, M.: Long-term trend of ventilation coefficient over Delhi and its potential impacts on air quality, Remote Sens. Appl. Soc. Environ., 15, 100234, https://doi.org/10.1016/J.RSASE.2019.05.003, 2019.

Sahu, L. K. and Saxena, P.: High time and mass resolved PTR-TOF-MS measurements of VOCs at an urban site of India during winter: Role of anthropogenic, biomass burning, biogenic and photochemical sources, Atmos. Res., 164–165, 84–94, https://doi.org/10.1016/J.ATMOSRES.2015.04.021, 2015.

Sahu, L. K., Tripathi, N., and Yadav, R.: Contribution of biogenic and photochemical sources to ambient VOCs during winter to summer transition at a semi-arid urban site in India, Environ. Pollut., 229, 595–606, https://doi.org/10.1016/J.ENVPOL.2017.06.091, 2017.

Sawlani, R., Agnihotri, R., Sharma, C., Patra, P. K., Dimri, A. P., Ram, K., and Verma, R. L.: The severe Delhi SMOG of 2016: A case of delayed crop residue burning, coincident firecracker emissions, and atypical meteorology, Atmos. Pollut. Res., 10, 868–879, https://doi.org/10.1016/j.apr.2018.12.015, 2019.

Schindelka, J., Iinuma, Y., Hoffmann, D., and Herrmann, H.: Sulfate radical-initiated formation of isoprene-derived organosulfates in atmospheric aerosols, Faraday Discuss., 165, 237–259, https://doi.org/10.1039/c3fd00042g, 2013.

Schnell, J. L., Naik, V., Horowitz, L. W., Paulot, F., Mao, J., Ginoux, P., Zhao, M., and Ram, K.: Exploring the relationship between surface $PM_{2.5}$ and meteorology in Northern India, Atmos. Chem. Phys., 18, 10157–10175, https://doi.org/10.5194/acp-18-10157-2018, 2018.

Sharma, S. K. and Mandal, T. K.: Chemical composition of fine mode particulate matter ($PM_{2.5}$) in an urban area of Delhi, India and its source apportionment, Urban Clim., 21, 106–122, https://doi.org/10.1016/j.uclim.2017.05.009, 2017.

Sheesley, R. J., Kirillova, E., Andersson, A., Krusa, M., Praveen, P. S., Budhavant, K., Safai, P. D., Rao, P. S. P., and Gustafsson, O.: Year-round radiocarbon-based source apportionment of carbonaceous aerosols at two background sites in South Asia, J. Geophys. Res.-Atmos., 117, D10, https://doi.org/10.1029/2011JD017161, 2012.

Shivani, R. G., Sharma, S. K., and Mandal, T. K.: Seasonal variation, source apportionment and source attributed health risk of fine carbonaceous aerosols over National Capital Region, India, Chemosphere, 237, 124500, https://doi.org/10.1016/j.chemosphere.2019.124500, 2019.

Simon, M., Dada, L., Heinritzi, M., Scholz, W., Stolzenburg, D., Fischer, L., Wagner, A. C., Kürten, A., Rörup, B., He, X.-C., Almeida, J., Baalbaki, R., Baccarini, A., Bauer, P. S., Beck, L., Bergen, A., Bianchi, F., Bräkling, S., Brilke, S., Caudillo, L., Chen, D., Chu, B., Dias, A., Draper, D. C., Duplissy, J., El-Haddad, I., Finkenzeller, H., Frege, C., Gonzalez-Carracedo, L., Gordon, H., Granzin, M., Hakala, J., Hofbauer, V., Hoyle, C. R., Kim, C., Kong, W., Lamkaddam, H., Lee, C. P., Lehtipalo, K., Leiminger, M., Mai, H., Manninen, H. E., Marie, G., Marten, R., Mentler, B., Molteni, U., Nichman, L., Nie, W., Ojdanic, A., Onnela, A., Partoll, E., Petäjä, T., Pfeifer, J., Philippov, M., Quéléver, L. L. J., Ranjithkumar, A., Rissanen, M. P., Schallhart, S., Schobesberger, S., Schuchmann, S., Shen, J., Sipilä, M., Steiner, G., Stozhkov, Y., Tauber, C., Tham, Y. J., Tomé, A. R., Vazquez-Pufleau, M., Vogel, A. L., Wagner, R., Wang, M., Wang, D. S., Wang, Y., Weber, S. K., Wu, Y., Xiao, M., Yan, C., Ye, P., Ye, Q., Zauner-Wieczorek, M., Zhou, X., Baltensperger, U., Dommen, J., Flagan, R. C., Hansel, A., Kulmala, M., Volkamer, R., Winkler, P. M., Worsnop, D. R., Donahue, N. M., Kirkby, J., and Curtius, J.: Molecular understanding of new-

particle formation from α-pinene between −50 and +25 °C, Atmos. Chem. Phys., 20, 9183–9207, https://doi.org/10.5194/acp-20-9183-2020, 2020.

Sindelarova, K., Granier, C., Bouarar, I., Guenther, A., Tilmes, S., Stavrakou, T., Müller, J.-F., Kuhn, U., Stefani, P., and Knorr, W.: Global data set of biogenic VOC emissions calculated by the MEGAN model over the last 30 years, Atmos. Chem. Phys., 14, 9317–9341, https://doi.org/10.5194/acp-14-9317-2014, 2014.

Singh, B. P., Kumar, K., and Jain, V. K.: Source identification and health risk assessment associated with particulate- and gaseous-phase PAHs at residential sites in Delhi, India, Air Qual. Atmos. Heal., 14, 1505–1521, https://doi.org/10.1007/S11869-021-01035-5, 2021.

Singh, D. P., Gadi, R., and Mandal, T. K.: Characterization of Gaseous and Particulate Polycyclic Aromatic Hydrocarbons in Ambient Air of Delhi, India, Polycycl. Aromat. Compd., 32, 556–579, https://doi.org/10.1080/10406638.2012.683230, 2012.

Sinha, V., Kumar, V., and Sarkar, C.: Chemical composition of pre-monsoon air in the Indo-Gangetic Plain measured using a new air quality facility and PTR-MS: high surface ozone and strong influence of biomass burning, Atmos. Chem. Phys., 14, 5921–5941, https://doi.org/10.5194/acp-14-5921-2014, 2014.

Spolnik, G., Wach, P., Rudzinski, K. J., Skotak, K., Danikiewicz, W., and Szmigielski, R.: Improved UHPLC-MS/MS Methods for Analysis of Isoprene-Derived Organosulfates, Anal. Chem., 90, 3416–3423, https://doi.org/10.1021/acs.analchem.7b05060, 2018.

Squires, F. A., Nemitz, E., Langford, B., Wild, O., Drysdale, W. S., Acton, W. J. F., Fu, P., Grimmond, C. S. B., Hamilton, J. F., Hewitt, C. N., Hollaway, M., Kotthaus, S., Lee, J., Metzger, S., Pingintha-Durden, N., Shaw, M., Vaughan, A. R., Wang, X., Wu, R., Zhang, Q., and Zhang, Y.: Measurements of traffic-dominated pollutant emissions in a Chinese megacity, Atmos. Chem. Phys., 20, 8737–8761, https://doi.org/10.5194/acp-20-8737-2020, 2020.

Stewart, G. J., Acton, W. J. F., Nelson, B. S., Vaughan, A. R., Hopkins, J. R., Arya, R., Mondal, A., Jangirh, R., Ahlawat, S., Yadav, L., Sharma, S. K., Dunmore, R. E., Yunus, S. S. M., Hewitt, C. N., Nemitz, E., Mullinger, N., Gadi, R., Sahu, L. K., Tripathi, N., Rickard, A. R., Lee, J. D., Mandal, T. K., and Hamilton, J. F.: Emissions of non-methane volatile organic compounds from combustion of domestic fuels in Delhi, India, Atmos. Chem. Phys., 21, 2383–2406, https://doi.org/10.5194/acp-21-2383-2021, 2021a.

Stewart, G. J., Nelson, B. S., Acton, W. J. F., Vaughan, A. R., Farren, N. J., Hopkins, J. R., Ward, M. W., Swift, S. J., Arya, R., Mondal, A., Jangirh, R., Ahlawat, S., Yadav, L., Sharma, S. K., Yunus, S. S. M., Hewitt, C. N., Nemitz, E., Mullinger, N., Gadi, R., Sahu, L. K., Tripathi, N., Rickard, A. R., Lee, J. D., Mandal, T. K., and Hamilton, J. F.: Emissions of intermediate-volatility and semi-volatile organic compounds from domestic fuels used in Delhi, India, Atmos. Chem. Phys., 21, 2407–2426, https://doi.org/10.5194/acp-21-2407-2021, 2021b.

Stewart, G. J., Nelson, B. S., Drysdale, W. S., Acton, W. J. F., Vaughan, A. R., Hopkins, J. R., Dunmore, R. E., Hewitt, C. N., Nemitz, E., Mullinger, N., Langford, B., Shivani, Reyes-Villegas, E., Gadi, R., Rickard, A. R., Lee, J. D., and Hamilton, J. F.: Sources of non-methane hydrocarbons in surface air in Delhi, India, Faraday Discuss., 226, 409–431, https://doi.org/10.1039/D0FD00087F, 2021c.

Surratt, J. D., Murphy, S. M., Kroll, J. H., Ng, N. L., Hildebrandt, L., Sorooshian, A., Szmigielski, R., Vermeylen, R., Maenhaut, W., Claeys, M., Flagan, R. C., and Seinfeld, J. H.: Chemical composition of secondary organic aerosol formed from the photooxidation of isoprene, J. Phys. Chem. A, 110, 9665–9690, https://doi.org/10.1021/jp061734m, 2006.

Surratt, J. D., Kroll, J. H., Kleindienst, T. E., Edney, E. O., Claeys, M., Sorooshian, A., Ng, N. L., Offenberg, J. H., Lewandowski, M., Jaoui, M., Flagan, R. C., and Seinfeld, J. H.: Evidence for Organosulfates in Secondary Organic Aerosol, Environ. Sci. Technol., 41, 517–527, https://doi.org/10.1021/es062081q, 2007.

Surratt, J. D., Gómez-González, Y., Chan, A. W. H., Vermeylen, R., Shahgholi, M., Kleindienst, T. E., Edney, E. O., Offenberg, J. H., Lewandowski, M., Jaoui, M., Maenhaut, W., Claeys, M., Flagan, R. C., and Seinfeld, J. H.: Organosulfate Formation in Biogenic Secondary Organic Aerosol, J. Phys. Chem. A, 112, 8345–8378, https://doi.org/10.1021/jp802310p, 2008.

Surratt, J. D., Chan, A. W. H., Eddingsaas, N. C., Chan, M., Loza, C. L., Kwan, A. J., Hersey, S. P., Flagan, R. C., Wennberg, P. O., and Seinfeld, J. H.: Reactive intermediates revealed in secondary organic aerosol formation from isoprene, P. Natl. Acad. Sci. USA, 107, 6640–6645, https://doi.org/10.1073/pnas.0911114107, 2010.

Szidat, S., Jenk, T. M., Gäggeler, H. W., Synal, H. A., Fisseha, R., Baltensperger, U., Kalberer, M., Samburova, V., Wacker, L., Saurer, M., Schwikowski, M., and Hajdas, I.: Source apportionment of aerosols by ^{14}C measurements in different carbonaceous particle fractions, in: Radiocarbon, University of Arizona, vol. 46, pp. 475–484, 2004.

Takeuchi, M. and Ng, N. L.: Chemical composition and hydrolysis of organic nitrate aerosol formed from hydroxyl and nitrate radical oxidation of α-pinene and β-pinene, Atmos. Chem. Phys., 19, 12749–12766, https://doi.org/10.5194/acp-19-12749-2019, 2019.

Wagner, P. and Kuttler, W.: Biogenic and anthropogenic isoprene in the near-surface urban atmosphere – A case study in Essen, Germany, Sci. Total Environ., 475, 104–115, https://doi.org/10.1016/J.SCITOTENV.2013.12.026, 2014.

Wang, J. L., Chew, C., Chang, C. Y., Liao, W. C., Lung, S. C. C., Chen, W. N., Lee, P. J., Lin, P. H., and Chang, C. C.: Biogenic isoprene in subtropical urban settings and implications for air quality, Atmos. Environ., 79, 369–379, https://doi.org/10.1016/J.ATMOSENV.2013.06.055, 2013.

Wang, X., Hayeck, N., Brüggemann, M., Yao, L., Chen, H., Zhang, C., Emmelin, C., Chen, J., George, C., and Wang, L.: Chemical Characteristics of Organic Aerosols in Shanghai: A Study by Ultrahigh-Performance Liquid Chromatography Coupled With Orbitrap Mass Spectrometry, J. Geophys. Res.-Atmos., 122, 11703–11722, https://doi.org/10.1002/2017JD026930, 2017.

Wang, X. K., Rossignol, S., Ma, Y., Yao, L., Wang, M. Y., Chen, J. M., George, C., and Wang, L.: Molecular characterization of atmospheric particulate organosulfates in three megacities at the middle and lower reaches of the Yangtze River, Atmos. Chem. Phys., 16, 2285–2298, https://doi.org/10.5194/acp-16-2285-2016, 2016.

Wang, Y., Hu, M., Guo, S., Wang, Y., Zheng, J., Yang, Y., Zhu, W., Tang, R., Li, X., Liu, Y., Le Breton, M., Du, Z., Shang,

D., Wu, Y., Wu, Z., Song, Y., Lou, S., Hallquist, M., and Yu, J.: The secondary formation of organosulfates under interactions between biogenic emissions and anthropogenic pollutants in summer in Beijing, Atmos. Chem. Phys., 18, 10693–10713, https://doi.org/10.5194/acp-18-10693-2018, 2018.

Wang, Y., Tong, R., and Yu, J. Z.: Chemical Synthesis of Multifunctional Air Pollutants: Terpene-Derived Nitrooxy Organosulfates, Environ. Sci. Technol., 55, acs.est.1c00348, https://doi.org/10.1021/acs.est.1c00348, 2021a.

Wang, Y., Zhao, Y., Wang, Y., Yu, J.-Z., Shao, J., Liu, P., Zhu, W., Cheng, Z., Li, Z., Yan, N., and Xiao, H.: Organosulfates in atmospheric aerosols in Shanghai, China: seasonal and interannual variability, origin, and formation mechanisms, Atmos. Chem. Phys., 21, 2959–2980, https://doi.org/10.5194/acp-21-2959-2021, 2021b.

Wennberg, P. O., Bates, K. H., Crounse, J. D., Dodson, L. G., McVay, R. C., Mertens, L. A., Nguyen, T. B., Praske, E., Schwantes, R. H., Smarte, M. D., St Clair, J. M., Teng, A. P., Zhang, X., and Seinfeld, J. H.: Gas-Phase Reactions of Isoprene and Its Major Oxidation Products, Chem. Rev., 118, 3337–3390, https://doi.org/10.1021/acs.chemrev.7b00439, 2018.

Wozniak, A. S., Bauer, J. E., and Dickhut, R. M.: Characteristics of water-soluble organic carbon associated with aerosol particles in the eastern United States, Atmos. Environ., 46, 181–188, https://doi.org/10.1016/j.atmosenv.2011.10.001, 2012.

Xu, J., Song, S., Harrison, R. M., Song, C., Wei, L., Zhang, Q., Sun, Y., Lei, L., Zhang, C., Yao, X., Chen, D., Li, W., Wu, M., Tian, H., Luo, L., Tong, S., Li, W., Wang, J., Shi, G., Huangfu, Y., Tian, Y., Ge, B., Su, S., Peng, C., Chen, Y., Yang, F., Mihajlidi-Zelić, A., Đordević, D., Swift, S. J., Andrews, I., Hamilton, J. F., Sun, Y., Kramawijaya, A., Han, J., Saksakulkrai, S., Baldo, C., Hou, S., Zheng, F., Daellenbach, K. R., Yan, C., Liu, Y., Kulmala, M., Fu, P., and Shi, Z.: An interlaboratory comparison of aerosol inorganic ion measurements by ion chromatography: implications for aerosol pH estimate, Atmos. Meas. Tech., 13, 6325–6341, https://doi.org/10.5194/amt-13-6325-2020, 2020.

Xu, L., Guo, H., Boyd, C. M., Klein, M., Bougiatioti, A., Cerully, K. M., Hite, J. R., Isaacman-VanWertz, G., Kreisberg, N. M., Knote, C., Olson, K., Koss, A., Goldstein, A. H., Hering, S. V., Gouw, J. de, Baumann, K., Lee, S.-H., Nenes, A., Weber, R. J., and Ng, N. L.: Effects of anthropogenic emissions on aerosol formation from isoprene and monoterpenes in the southeastern United States, P. Natl. Acad. Sci. USA, 112, 37–42, https://doi.org/10.1073/PNAS.1417609112, 2015.

Yadav, A. K., Sarkar, S., Jyethi, D. S., Rawat, P., Aithani, D., Siddiqui, Z., and Khillare, P. S.: Fine Particulate Matter Bound Polycyclic Aromatic Hydrocarbons and Carbonaceous Species in Delhi's Atmosphere: Seasonal Variation, Sources, and Health Risk Assessment, Aerosol Sci. Eng., 5, 193–213, https://doi.org/10.1007/S41810-021-00094-6, 2021.

Yee, L. D., Isaacman-VanWertz, G., Wernis, R. A., Kreisberg, N. M., Glasius, M., Riva, M., Surratt, J. D., de Sá, S. S., Martin, S. T., Alexander, M. L., Palm, B. B., Hu, W., Campuzano-Jost, P., Day, D. A., Jimenez, J. L., Liu, Y., Misztal, P. K., Artaxo, P., Viegas, J., Manzi, A., de Souza, R. A. F., Edgerton, E. S., Baumann, K., and Goldstein, A. H.: Natural and Anthropogenically Influenced Isoprene Oxidation in Southeastern United States and Central Amazon, Environ. Sci. Technol., 54, 5980–5991, https://doi.org/10.1021/acs.est.0c00805, 2020.

Zhang, H., Yee, L. D., Lee, B. H., Curtis, M. P., Worton, D. R., Isaacman-VanWertz, G., Offenberg, J. H., Lewandowski, M., Kleindienst, T. E., Beaver, M. R., Holder, A. L., Lonneman, W. A., Docherty, K. S., Jaoui, M., Pye, H. O. T., Hu, W., Day, D. A., Campuzano-Jost, P., Jimenez, J. L., Guo, H., Weber, R. J., De Gouw, J., Koss, A. R., Edgerton, E. S., Brune, W., Mohr, C., Lopez-Hilfiker, F. D., Lutz, A., Kreisberg, N. M., Spielman, S. R., Hering, S. V., Wilson, K. R., Thornton, J. A., and Goldstein, A. H.: Monoterpenes are the largest source of summertime organic aerosol in the southeastern United States, P. Natl. Acad. Sci. USA, 115, 2038–2043, https://doi.org/10.1073/pnas.1717513115, 2018.

Zhang, H., Zhang, Y., Huang, Z., Acton, W. J. F., Wang, Z., Nemitz, E., Langford, B., Mullinger, N., Davison, B., Shi, Z., Liu, D., Song, W., Yang, W., Zeng, J., Wu, Z., Fu, P., Zhang, Q., and Wang, X.: Vertical profiles of biogenic volatile organic compounds as observed online at a tower in Beijing, J. Environ. Sci., 95, 33–42, https://doi.org/10.1016/J.JES.2020.03.032, 2020.

Zhao, D., Schmitt, S. H., Wang, M., Acir, I.-H., Tillmann, R., Tan, Z., Novelli, A., Fuchs, H., Pullinen, I., Wegener, R., Rohrer, F., Wildt, J., Kiendler-Scharr, A., Wahner, A., and Mentel, T. F.: Effects of NO_x and SO_2 on the secondary organic aerosol formation from photooxidation of a-pinene and limonene, Atmos. Chem. Phys., 18, 1611–1628, https://doi.org/10.5194/acp-18-1611-2018, 2018.

Zhao, D. F., Kaminski, M., Schlag, P., Fuchs, H., Acir, I.-H., Bohn, B., Häseler, R., Kiendler-Scharr, A., Rohrer, F., Tillmann, R., Wang, M. J., Wegener, R., Wildt, J., Wahner, A., and Mentel, Th. F.: Secondary organic aerosol formation from hydroxyl radical oxidation and ozonolysis of monoterpenes, Atmos. Chem. Phys., 15, 991–1012, https://doi.org/10.5194/acp-15-991-2015, 2015.

Zou, Y., Deng, X. J., Deng, T., Yin, C. Q., and Li, F.: One-year characterization and reactivity of isoprene and its impact on surface ozone formation at a suburban site in Guangzhou, China, Atmosphere-Basel, 10, 201, https://doi.org/10.3390/ATMOS10040201, 2019.